

REPORT DOCUMENTATION PAGE			Form Approved OMB No. 0704-0188	
Public reporting burden for this collection of information is estimated to average 1 hour per response, including the time for reviewing instructions, searching existing data sources, gathering and maintaining the data needed, and completing and reviewing the collection of information. Send comments regarding this burden estimate or any other aspect of this collection of information, including suggestions for reducing this burden, to Washington Headquarters Services, Directorate for Information Operations and Reports, 1215 Jefferson Davis Highway, Suite 1204, Arlington, VA 22202-4302, and to the Office of Management and Budget, Paperwork Reduction Project (0704-0188), Washington, DC 20503.				
1. AGENCY USE ONLY (Leave blank)		2. REPORT DATE 28.Oct.98		3. REPORT TYPE AND DATES COVERED THESIS
4. TITLE AND SUBTITLE SUBSTITUENT EFFECTS ON THE OPTICAL PROPERTIES OF FREE BASE A.B.Y.-TETRAPHENYLPORPHYRIN			5. FUNDING NUMBERS	
6. AUTHOR(S) 2D LT WOHLWEND KIRSTEN M				
7. PERFORMING ORGANIZATION NAME(S) AND ADDRESS(ES) WRIGHT STATE UNIVERSITY			8. PERFORMING ORGANIZATION REPORT NUMBER	
9. SPONSORING/MONITORING AGENCY NAME(S) AND ADDRESS(ES) THE DEPARTMENT OF THE AIR FORCE AFIT/CIA, BLDG 125 2950 P STREET WPAFB OH 45433			10. SPONSORING/MONITORING AGENCY REPORT NUMBER 98-107	
11. SUPPLEMENTARY NOTES				
12a. DISTRIBUTION AVAILABILITY STATEMENT Unlimited distribution In Accordance With AFI 35-205/AFIT Sup 1			12b. DISTRIBUTION CODE	
13. ABSTRACT (Maximum 200 words)				
<div data-bbox="345 1327 799 1449" data-label="Image"> </div> <div data-bbox="964 1325 1414 1415" data-label="Text"> <p>19981119 035</p> </div> <div data-bbox="940 1486 1305 1661" data-label="Text"> <p>DTIC QUALITY INSPECTED 4</p> </div>				
14. SUBJECT TERMS			15. NUMBER OF PAGES	
			16. PRICE CODE	
17. SECURITY CLASSIFICATION OF REPORT	18. SECURITY CLASSIFICATION OF THIS PAGE	19. SECURITY CLASSIFICATION OF ABSTRACT	20. LIMITATION OF ABSTRACT	

SUBSTITUENT EFFECTS ON THE OPTICAL PROPERTIES OF FREE BASE
 $\alpha,\beta,\gamma,\delta$ -TETRAPHENYLPORPHYRIN

A thesis submitted in partial fulfillment
of the requirements for the degree of
Master of Science

By

KIRSTEN MARIE WOHLWEND
B.S., United States Air Force Academy, 1997

1998
Wright State University

WRIGHT STATE UNIVERSITY
SCHOOL OF GRADUATE STUDIES

July 16, 1998

I HEREBY RECOMMEND THAT THE THESIS PREPARED UNDER MY SUPERVISION BY Kirsten Marie Wohlwend ENTITLED Substituent Effects on Optical Properties of Free Base α , β , γ , δ -Tetraphenylporphyrin BE ACCEPTED IN PARTIAL FULFILLMENT OF THE REQUIREMENTS FOR THE DEGREE OF Master of Science.

M. Paul Servé, Ph.D.
Thesis Director

M. Paul Servé, Ph.D.
Department Chair

Committee on Final Examination

William Feld, Ph.D.

David Grossie, Ph.D.

M. Paul Servé, Ph.D.

Joseph F. Thomas, Jr., Ph.D.
Dean, School of Graduate Studies

ABSTRACT

Wohlwend, Kirsten M., M.S. Department of Chemistry, Wright State University, 1998.
Substituent Effects on the Optical Properties of Free Base α , β , γ , δ -Tetraphenyl porphyrin

Optical limiting devices have gained importance as more laser threats have been developed. The purpose of this project was to study the optical properties of various substituted groups on TPP and use the information obtained to improve materials under investigation for potential use as optical limiting dyes. Compounds were obtained that had substituents added to the phenyl groups of free base tetraphenyl porphyrin. Absorption peak shifts, molar extinction coefficient, oscillator strength, fluorescence peak shifts, and fluorescence quantum yield were measured. Hammett sigma values were used to quantify the electron donating/withdrawing capacity of the substituents.

All optical properties studied showed a change in value based on the electron donating/withdrawing strength of the added substituent. Both absorbance and fluorescence spectra showed a red shift with more electron donating substituents. Molar extinction coefficient, oscillator strength and fluorescence quantum yield all showed an increase with more electron donating substituents. These trends can be used to design better optical limiting materials in the future.

The Hammett sigma was also used to determine the extent of resonance. When split into its resonance and inductive components and plotted against the optical properties studied, average values of approximately 69% resonance and 31% inductance were found.

TABLE OF CONTENTS

ABSTRACT.....	iii
LIST OF FIGURES.....	vii
LIST OF TABLES.....	ix
ACKNOWLEDGMENT.....	x
DEDICATION.....	xi
I. INTRODUCTION.....	1
OPTICAL LIMITING.....	2
PORPHYRIN BASICS AND THEORY.....	9
UV-VIS SPECTROPHOTOMETRY.....	17
MOLAR EXTINCTION COEFFICIENT.....	18
OSCILLATOR STRENGTH.....	18
FLUORESCENCE.....	19
QUANTUM YIELD.....	20
HAMMETT SIGMA.....	22
STERIC HINDRANCE.....	24
BASIC STATISTICS.....	25
PURPOSE.....	26
II. EXPERIMENTAL.....	27

COMPOUNDS USED.....	27
ABSORPTION λ_{max} SHIFT STUDY.....	29
MOLAR EXTINCTION COEFFICIENT.....	29
OSCILLATOR STRENGTH.....	30
FLUORESCENCE SHIFT STUDY.....	30
QUANTUM YIELD DETERMINATION.....	30
III. RESULTS AND DISCUSSION.....	32
PORPHYRIN ABSORPTION SPECTRA.....	32
ABSORPTION λ_{max} SHIFTING.....	33
MOLAR EXTINCTION COEFFICIENT.....	36
OSCILLATOR STRENGTH.....	39
FLUORESCENCE SPECTRA SHIFTING.....	42
QUANTUM YIELD.....	43
IV. CONCLUSION.....	46
APPENDICES	
A. Sample Q Band Absorption.....	49
B. Sample Fluorescence Spectra.....	56
REFERENCES.....	63
VITA.....	69

LIST OF FIGURES

<u>FIGURE</u>	<u>PAGE</u>
1. RSA Five Level Model.....	1
2. TPP Skeleton.....	2
3. Sample Diphenyl Polyenes.....	4
4. Sample Dithienyl Polyenes.....	4
5. RSA versus Saturable Absorption.....	6
6. Sample Polycyclic Aromatic Hydrocarbon Diones.....	7
7. Phthalocyanine Skeleton.....	7
8. Porphyrin Skeleton.....	8
9. Free Base Porphyrin.....	11
10. Metal Salt.....	11
11. Metal Salt Spectrum.....	11
12. Free Base Sample Spectrum.....	12
13. Porphyrin MOs.....	13
14. 16 Membered Conjugated System.....	14
15. 18 Membered Conjugated System.....	15
16. Possible Porphyrin Transitions.....	15
17. Beer-Lambert Law.....	17

18. Absorption/Emission Basics.....	20
19. Energy Minimized Structure of TPP.....	24
20. Absorption λ_{\max} Shift versus Hammett σ : Soret Band.....	34
21. Absorption λ_{\max} Shift versus Hammett σ : Q_x (0-0) Band.....	35
22. Absorption λ_{\max} Shift versus Combined σ : Soret Band.....	35
23. Absorption λ_{\max} Shift versus Combined σ : Q_x (0-0) Band.....	35
24. Soret Band Molar Extinction Coefficient versus Hammett σ	37
25. Q_x (0-0) Band Molar Extinction Coefficient versus Hammett σ	38
26. Soret Band Molar Extinction Coefficient versus Combined σ	38
27. Q_x (0-0) Band Molar Extinction Coefficient versus Combined σ	38
28. Oscillator Strength versus Hammett σ	40
29. Oscillator Strength versus Combined σ	41
30. Fluorescence versus Hammett σ	42
31. Fluorescence versus Combined σ	43
32. Quantum Yield versus Hammett σ	44
33. Quantum Yield versus Combined σ	45

LIST OF TABLES

<u>TABLE</u>	<u>PAGE</u>
1. Substituents Added.....	28
2. Hammett Sigma Values.....	29
3. Relative Q Band Intensities.....	32
4. Absorption Peak Shifts.....	33
5. Molar Extinction Coefficient.....	37
6. Calculated Oscillator Strength.....	40
7. Fluorescence Peak Shifts.....	42
8. Fluorescence Quantum Yield.....	44

ACKNOWLEDGMENT

The author wishes to extend her gratitude to Dr. M. Paul Servé for his guidance throughout this project as advisor. She also thanks Dr. William Feld and Dr. David Grossie for agreeing to be on the thesis committee.

The author would like to thank Dr. Tom Cooper, Dr. Weijie Su, and Ms. Donna Brandelik for their guidance, advice and support. She also thanks Dr. Kiet Nguyen for creating the energy minimized structure of TPP and all the others at the Air Force Research Laboratory, AFRL/MLPJ for their assistance with this project.

DEDICATION

To my husband, Christian, for his love and support. To my parents for everything they've done for me. Finally, to my niece Ashley, who's proving to me that the future is still bright.

I. INTRODUCTION

Optical limiters are devices containing dyes that undergo a nonlinear optical mechanism. Various nonlinear optical mechanisms can occur. These include nonlinear absorption, nonlinear refraction, induced scattering, and even phase transitions [1].

A reverse-saturable absorber (RSA) is a type of dye that can be used in an optical limiter. It undergoes nonlinear absorption and its excited states follow the five level model shown in Figure 1.

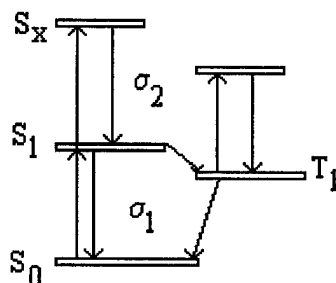


Figure 1. RSA Five Level Model

RSA occurs when the excited state absorption cross section is larger than the ground state cross section [1, 2]. To have good nonlinear absorption properties, a RSA must have a rapid crossover rate between $S_1 \rightarrow T_1$, a long internal conversion lifetime, and a long triplet lifetime [2]. Porphyrins, as a group, are good potential optical limiters because of their π electron systems. Perturbations of the π system with substituent groups vary the optical properties of the molecule. Being able to change the maximum wavelength of absorption

and the absorption band width of the molecule is important for optical limiting research. This allows molecules to be designed for specific laser threats.

Prior studies have shown that $\alpha,\beta,\gamma,\delta$ -tetraphenylporphyrin (TPP) undergoes RSA and is a good molecule to test for optical limiting [2]. Porphyrins can undergo many different reactions allowing for the synthesis of many derivatives. These can be used to determine structure-property relationships. This project is a study of the effect of attached substituent groups on the optical properties of TPP. A TPP skeleton is shown in Figure 2.

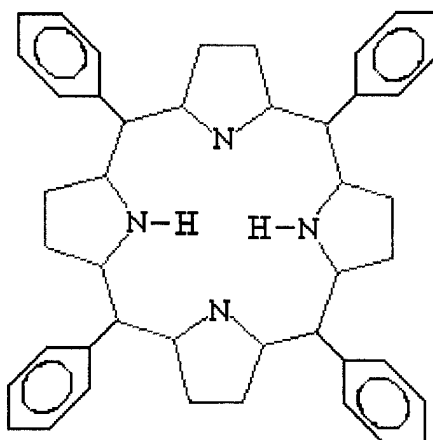


Figure 2. TPP Skeleton

OPTICAL LIMITING

Optical limiting is used when decreasing transmission with increasing excitation is needed. An important application for optical limiters is eye and sensor protection in optical systems, focal plane arrays and night vision systems [1,3]. All photonic sensors, including the eye, have a maximum intensity level they can withstand before damage occurs. Using an appropriate optical limiter can extend the dynamic range of the sensor and allow the sensor to operate under harsher conditions than normally possible [1].

Recently, much effort has been put into developing a passive optical limiter for this type of application.

A passive optical limiter is desired because it automatically responds to the laser pulse without requiring additional equipment or electronics. The other type, a dynamic limiter, uses active feedback. A photosensor is required to detect the pulse and multiple other components are needed to react to the pulse. These systems have many disadvantages including high complexity due to all the components and slow speeds because the components must communicate with each other. A passive optical limiter requires no added electronics. Without the added components, it is simple and its response to the pulse is just an inherent response of the dye, which may have a response time fast enough to block the first pulse of the threat laser [1].

This inherent response is a nonlinear mechanism. These mechanisms can include nonlinear absorption, nonlinear refraction, induced scattering and phase transitions. All optical nonlinearities can be classified as either instantaneous or accumulative. Optical limiters that rely on instantaneous nonlinearities usually work over a broad band while limiters that rely on accumulative nonlinearities have a narrow bandwidth of operation. Accumulative limiters can depend only on fluence as opposed to intensity and work on longer laser pulses. Instantaneous limiters require higher intensities and only work for short laser pulses [1].

One type of nonlinear absorption is two photon absorption (TPA). This is an instantaneous nonlinearity. An absorbed photon promotes an electron from its initial state to a virtual intermediate state. Then a second photon is absorbed that promotes the

electron to its final state. Compounds that exhibit TPA will react almost instantly to a pulse. The problem is that high intensities are needed for significant TPA to take place. Because intensity is energy density divided by pulse duration, short laser pulses are required for limiting with TPA in order to reach an energy density that would be high enough to damage an unprotected optical sensor. TPA alone is not enough for nanosecond or longer pulses [1].

Examples of materials that exhibit TPA include semiconductors, diphenyl polyenes, and dithienyl polyenes. Semiconductors have a narrow band gap that is being studied for infrared sensor protection [4-6]. Diphenyl polyenes, like the ones shown in Figure 3, have been reported to show TPA [3, 7-14].

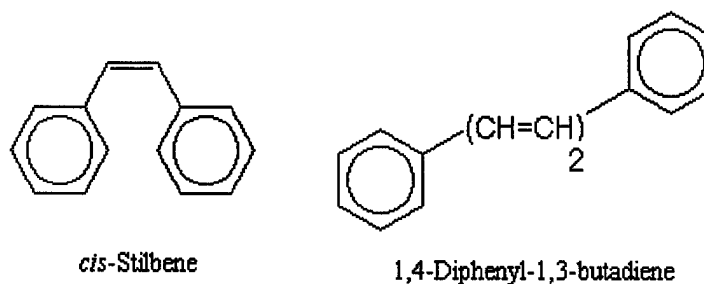


Figure 3. Sample Diphenyl Polyenes³

Dithienyl polyenes, including those shown in Figure 4, have also been reported to exhibit TPA [7, 11].

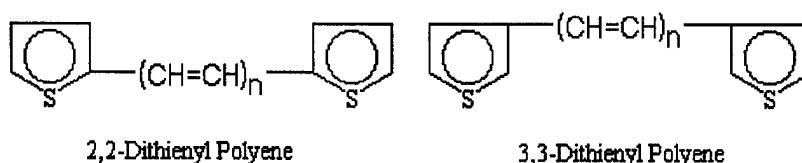


Figure 4. Sample Dithienyl Polyenes¹³

One of the reasons all of these compounds were studied for optical limiting is because of their π -electron systems. Conjugated π -electron systems tend to have larger optical nonlinearities and fast response times because it is relatively easy to polarize the extended π -electron clouds over large molecular distances [3, 15]. This polarizability can be manipulated even more by adding an electron donating group at one end of a molecule and an electron withdrawing group at the other end. This ability to "push-and-pull" the electron density makes conjugated π -electron systems attractive for optical limiting.

As stated before, TPA is instantaneous and thus is only useful with short pulses of high energy. Not all threats correspond to those conditions. Thus, an optical limiter with an accumulative nonlinearity would be useful. One type of optical limiter with accumulative nonlinearity is one that exhibits reverse saturable absorption (RSA). It was first reported by Guiliano and Hess in 1967 [16]. They, in addition to many other researchers, were investigating various dyes for use in the newly developed field of lasers. Guiliano and Hess saw that some of the dyes they were studying darkened at high intensities instead of bleaching to transparency. The darkening was caused by RSA. Its mechanism is described by the five level model shown in Figure 1. RSA occurs when the excited state absorption cross section, σ_2 , is larger than the ground state absorption cross section, σ_1 . The opposite, saturable absorption, causes bleaching at high incident intensity [1]. The darkening and bleaching are illustrated in Figure 5.

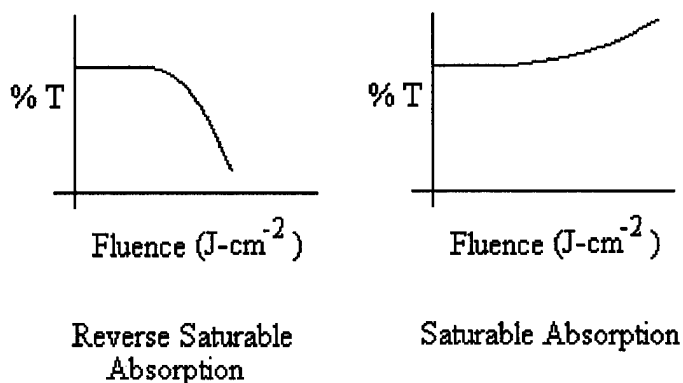


Figure 5. RSA versus Saturable Absorption

For highest efficiency, the crossover rate from $S_1 \rightarrow T_1$ should be rapid, both the internal conversion lifetime and the triplet lifetime should be long, and the triplet quantum yield should be large [1, 2, 17]. This allows for the population of the triplet state and keeps it populated throughout the pulse.

As with TPA, many different classes of compounds have been studied that undergo RSA. These include fullerenes, polycyclic aromatic hydrocarbon diones, phthalocyanines and porphyrins [1, 16-39].

Fullerenes, especially C_{60} , were studied in the early 1990s because the optical limiting performance was competitive with other optical limiting materials of the time [18-21]. Bentivegna *et al* even showed that the C_{60} still exhibited RSA when incorporated in solid xerogel matrices, which meant C_{60} was versatile [22]. C_{60} is now the organic optical limiter standard for RSA. However, at high fluences C_{60} did not work as well as hoped and other classes of compounds were studied [23].

Polycyclic aromatic hydrocarbon diones, shown in Figure 6, have been studied by Natarajan *et al* for optical limiting since the mid 1990's.

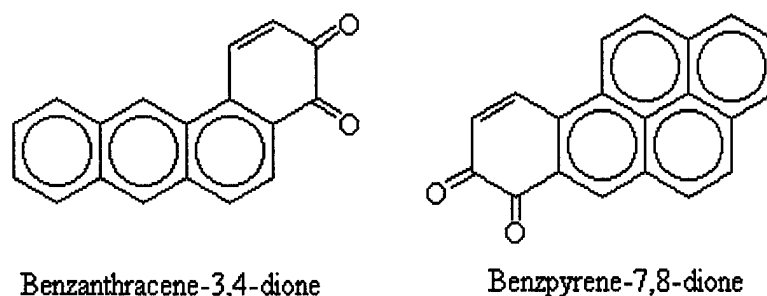


Figure 6. Sample Polycyclic Aromatic Hydrocarbon Diones

These were studied because of the high triplet quantum yields that were previously reported [24, 25]. They were found to show better overall limiting for the same initial transmittance when compared to C_{60} [17].

Conjugated π -electron systems improve the optical limiting performance for compounds that exhibit RSA as well. Phthalocyanines, with their conjugated π -electron system, were studied for optical limiting by Van Stryland and Perry [26-28]. A phthalocyanine is shown in Figure 7.

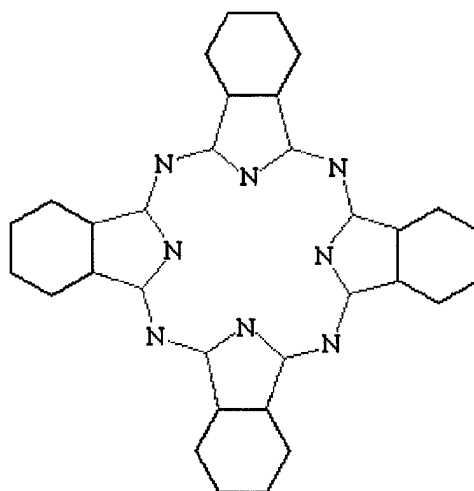


Figure 7. Phthalocyanine Skeleton

Unfortunately, there are a few problems with phthalocyanines. They have low solubility and they can undergo a relatively small number of reactions. While not being very reactive may not seem to be a big problem, when trying to design an optical limiter for a specific sensor, having the ability to make small changes to the structure of the molecule in order to make the best limiter possible is important. Thus, a related class of compounds, porphyrins, have been studied.

The basic porphyrin skeleton is shown in Figure 8.

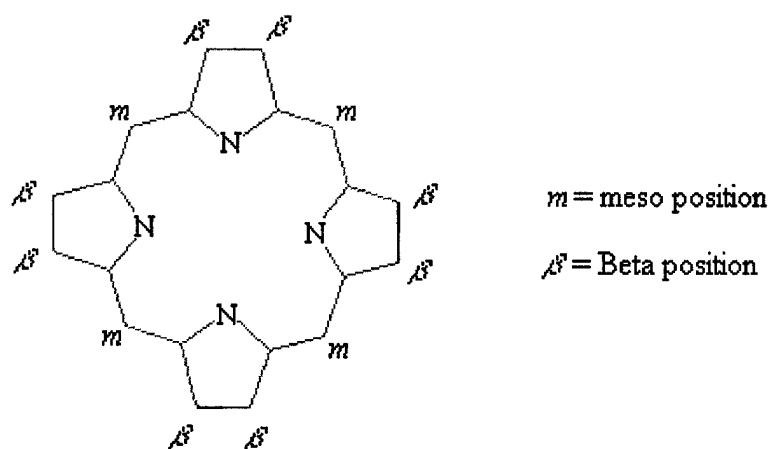


Figure 8. Porphyrin Skeleton

Porphyrins have a conjugated π -electron system, similar to phthalocyanines. Unlike phthalocyanines, porphyrins can undergo many reactions with greater ease. While there is no one solvent that can solubilize all porphyrins, as a class they are much more soluble than phthalocyanines.

In 1985, Blau *et al* showed that free base tetraphenyl porphyrins and their metal salts undergo RSA [29]. However, using porphyrins for optical limiting was not really examined in detail until the mid 1990's.

Halogenated porphyrins are one type of porphyrin currently being studied for optical limiting applications. In 1992, Bonnett *et al* found that adding even just one bromine atom at any beta position in Figure 8 resulted in an improvement of the crossover rate from $S_1 \rightarrow T_1$ to almost unity [30]. Many other studies using different halogens and various transition metals to create the metal salt were completed [30-37]. However, these studies were focused more on their use in catalysis and not on optical limiting. In 1996, Tang *et al* finished their initial study of the nonlinear absorption of brominated porphyrins and found that many of their compounds outperformed C_{60} [38]. In 1998, Su reported more in depth studies of the RSA for brominated porphyrins [2].

Because of the good initial results of the porphyrins modified at the beta positions of Figure 8, other studies of porphyrins have been completed involving substitutions to the meso positions. Optical limiting in meso-alkynyl porphyrins was reported by Tang's group in 1997 [39]. Concurrently, Su reported optical properties of various meso substituted porphyrins [40]. Based on those results, many compounds, including TPP, were found to have good enough initial results to warrant further studies.

PORPHYRIN BASICS AND THEORY

While the five level model for RSA is applicable to the porphyrins studied, basic porphyrin theory goes back to Gouterman's four orbital model [41-44]. Gouterman's initial porphyrin theory was published in 1959. Gouterman used a simple Hückel model

which allowed for variations in the porphyrin skeleton and then added a cyclic polyene model to incorporate electron interaction effects. This theory predicted intensity relationships based on the degree of degeneracy of the top filled molecular orbitals. It can be extended to explain TPP properties because the TPP molecules studied have four identical phenyl groups. In 1985, Balke *et al* determined that when four identical phenyl substituents are added in the meso positions of porphyrin, the system is forced into direct conjugation [45]. Because of this, the effects of identical substituents on all four phenyl groups can be studied.

Studying effects of substituents on the phenyl groups instead of the effects of the same substituents substituted directly on the porphyrin basic skeleton is important because it is easier to synthesize the variations of TPP. Ease of synthesis is important in creating usable optical limiting devices because they must be economically feasible, both in direct monetary terms and in terms of time invested. While the compounds used in this study had low yields compared to many organic reactions, their synthesis was still much easier than a corresponding synthesis directly on the porphyrin skeleton. The basic TPP synthesis was based on the work of Adler, which was modified based on the specific porphyrin desired [46-49].

Before going into Gouterman's four orbital model in more depth, the difference between a free base porphyrin and a metal salt should be discussed. The free base porphyrin, shown in Figure 9, has hydrogen attached to the nitrogens on rings 2 and 4. This causes the molecule to have D_{2h} symmetry. The metal salt, shown in Figure 10, has a

metal in the center of the molecule. Because the two hydrogens are no longer there, the molecule now has D_{4h} symmetry.

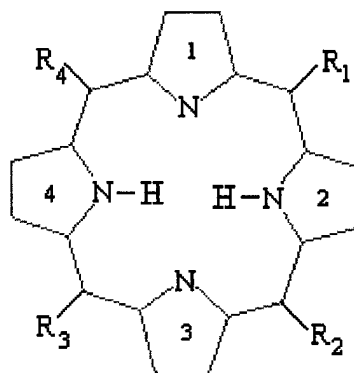


Figure 9. Free Base Porphyrin

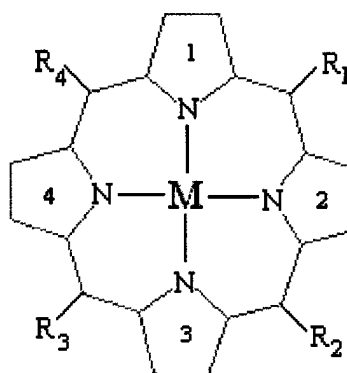


Figure 10. Metal Salt

A typical metal salt spectrum is shown in Figure 11. A typical free base spectrum is shown in Figure 12. The strong UV band is called the B or Soret band. The bands in the visible region are the Q bands [41]. The Q bands were multiplied by 5 so that they could be seen on the plots.

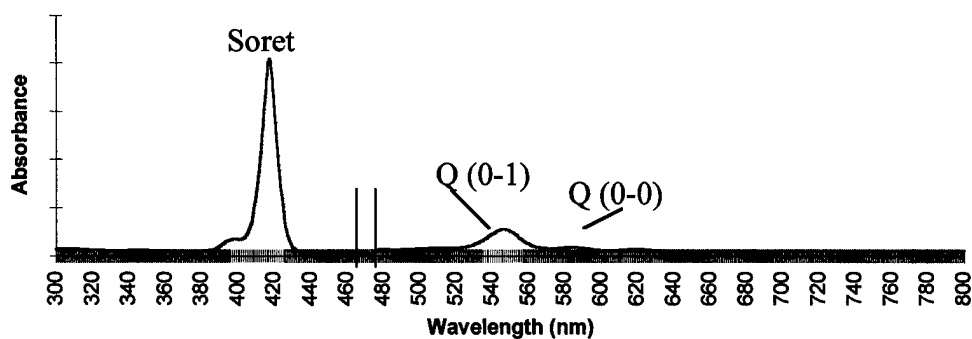


Figure 11. Metal Salt Spectrum⁵⁰

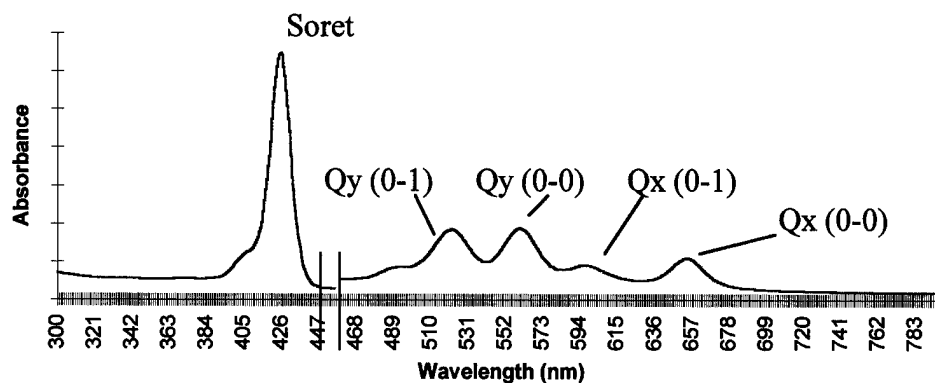


Figure 12. Free Base Sample Spectrum

The Q (0-1) band is due to mixing of vibrational and electronic motions called vibronic interaction. It borrows intensity from the allowed Soret transition [42]. The free base porphyrin spectrum shows a splitting of the Q bands compared to the metal salt. These are labeled $Q_x(0,0)$ and $Q_y(0,0)$. Each have a vibronic overtone band labeled $Q_x(0-1)$ and $Q_y(0-1)$. This Q band splitting has to do with symmetry differences between the free base and metal salt and will be discussed momentarily.

The simple Hückel model was the first model to involve the shape of the porphyrin molecule in its calculations [44]. The MOs calculated are shown in Figure 13.

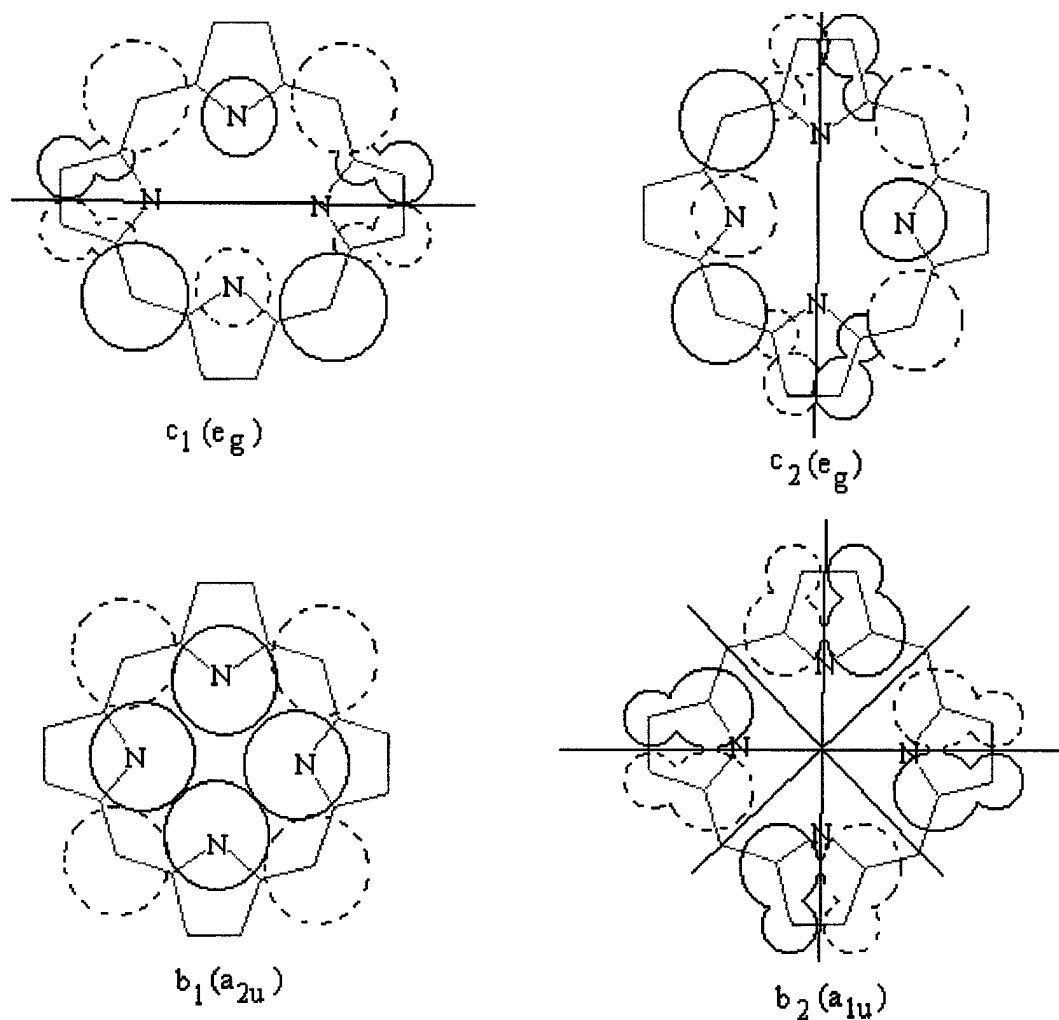


Figure 13. Porphyrin MOs⁴⁴

Longuet-Higgins *et al* found that the highest occupied molecular orbitals, the HOMOs, were $3a_{2u}(\pi)$ and $1a_{1u}(\pi)$ while the two degenerate $4e_g(\pi^*)$ were the lowest unoccupied molecular orbitals, the LUMOs [51]. The $3a_{2u} \rightarrow 4e_g$ transition was calculated to be lower energy than the $1a_{1u} \rightarrow 4e_g$ transition. Therefore, the Q bands come from the first transition while the B band comes from the second transition. While this model did give an idea of

where the bands should occur, it predicted they would be equal intensity. Thus, this model only helped by giving an idea of what changes to the porphyrin skeleton will do to the shifting of the bands.

To account for electron interactions, a cyclic polyene model is used. The metal salt can be described as a 16 membered cyclic polyene with 18 π electrons. This inner 16 membered conjugated system can be seen in Figure 14 [52].

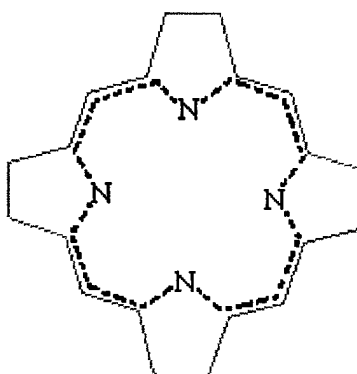


Figure 14. 16 Membered Conjugated System⁵²

For the symmetrical metal salt, the x and y components of the molecule are the same thus the Q_x and Q_y spectral bands are degenerate. The metal π electrons interact with the a_{2u} orbital and conjugates with the π electrons in the ring [43]. The transitions seen are $a_{2u} \rightarrow e_g$ and $a_{1u} \rightarrow e_g$ transitions. The energy associated with this transition is in the right region for the porphyrin spectrum, thus this simple model works.

In order to describe the splitting of the Q band seen in the free base porphyrin, an 18 membered cyclic polyene with 18 π electrons must be used [43]. This 18 membered ring is shown in Figure 15 [44].

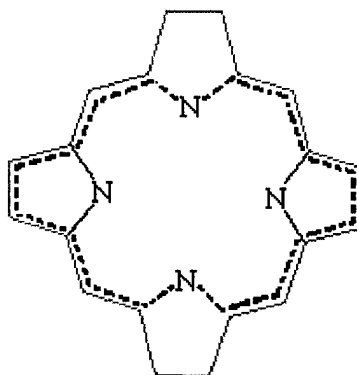


Figure 15. 18 Membered Conjugated System⁴⁴

The four orbital model tried to take the best from each of these previous models and make it general enough to explain both metal salts with their high degree of symmetry and free base porphyrins with their lower symmetry. To accommodate the difference in symmetry between the free base and the metal salt, the MOs shown in Figure 13 were relabeled using b_1 and b_2 for the HOMOs, while the LUMOs were relabeled c_1 and c_2 . Using the b and c labels, all the possible transitions between the b and c orbitals are shown in Figure 16 [41]

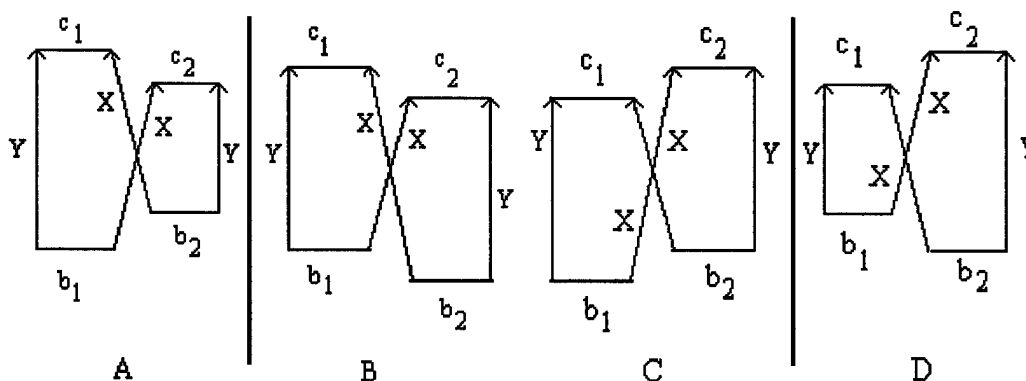


Figure 16. Possible Porphyrin Transitions⁴¹

This study was of free base porphyrins so it is necessary to determine which of the four transitions above occur for the free base. The orbital energies change as the porphyrin goes from the metal salt to the free base. This can be shown by looking at electron density. Orbital c_1 has its electron density more on the nitrogens of rings 1 and 3 while orbital c_2 has the opposite. Assuming the protons add on the x axis, they are added to the nitrogens on rings 2 and 4 [41]. This lowers the energy of orbital c_2 when compared to orbital c_1 , thus Figures 16 A or B would be correct. In 1961, Gouterman reported that b_2 is higher than b_1 for free base porphyrin [41]. He based this conclusion on the spectrum shown by the free base porphyrin. Thus, Figure 16 A is true for free base porphyrin.

The Q band intensities are based on the relative energies of transitions from the HOMO (b level) to the LUMO (c level). If the transition energies are equal, the Q (0-0) bands have no intensity and as the transition energies start to vary, the Q (0-0) bands gain intensity [41]. This can be used to predict how porphyrin spectra should appear.

In the HOMOs of TPP, the phenyl groups affect orbital b_1 the most. Adding the four phenyl groups to form TPP from free base porphyrin adds electron density to orbital b_1 raising it in relation to orbital b_2 . Raising this orbital causes a larger relative difference between the transitions for Q_x and Q_y which causes Q_x (0-0) and Q_y (0-0) to gain strength relative to free base porphyrin. Electron donating groups substituted on the phenyl rings would also raise the energy of orbital b_1 while electron withdrawing groups would decrease the energy of the orbital [53].

UV-VIS SPECTROPHOTOMETRY

For optical limiting applications, UV-VIS absorption is important. Absorption maxima set the limits on the useful range of the dye being studied. Improving an optical limiting device would involve making it have an absorption maximum at the proper wavelength to protect against the specific laser threat. Another improvement is to increase the bandwidth of the absorption. This would allow the limiter to protect against a wider threat range.

The equation describing UV-VIS spectra is the Beer-Lambert Law, shown as equation (1),

$$A = abc \quad \text{Equation (1)}$$

where A is absorption, a is absorptivity, b is sample thickness and c is sample concentration in moles L^{-1} . Absorptivity is constant for each compound but is dependent on wavelength and is called molar absorptivity or molar extinction coefficient, ϵ , when its units are $L \text{ mol}^{-1} \text{ cm}^{-1}$. The Beer-Lambert law is linear over a certain range of concentrations and then becomes nonlinear as concentration increases. This can be seen in Figure 17.

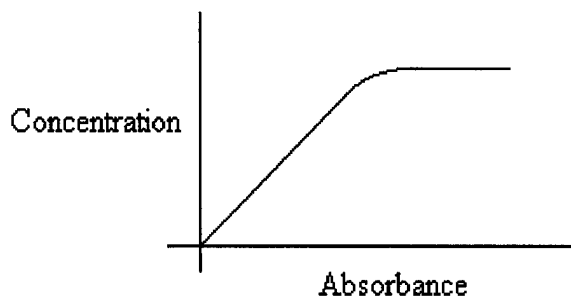


Figure 17. Beer-Lambert Law

Molecular interactions are what cause the nonlinearity at higher concentrations. The Beer-Lambert law requires dilute concentrations so that each molecule behaves independently of the others. When the concentration is no longer in the linear range, the equation cannot be used to determine molar extinction coefficient.

MOLAR EXTINCTION COEFFICIENT

The molar extinction coefficient of a compound defines the probability that an electronic transition will take place in a known concentration of the compound [54]. It is a physical property describing the absorbed radiation of compounds and can thus be used to quantitatively compare promising molecules. It is solvent dependent [55].

In optical limiting, a high molar extinction coefficient is desired. A dye with a low ϵ would require a long path length for it to be effective against a laser threat. For porphyrins, the Soret band has molar extinction coefficients in the 10^5 range while the weak $Q_x(0-0)$ band has molar extinction coefficients in the 10^3 range [31, 45, 56, 57]. These values are high enough for porphyrins to be considered for optical limiting applications.

OSCILLATOR STRENGTH

Another calculation that can be used is oscillator strength. Oscillator strength is the excitation probability of an electron in a nuclear framework [58]. It is a theoretical quantity that is defined by equation 2,

$$f \equiv 4.3 \cdot 10^{-9} \int \epsilon \, d\nu \quad \text{Equation (2)}$$

where ϵ is the molar extinction coefficient and ν is the energy in wavenumbers of the absorption in question [58]. Oscillator strength can be approximated using equation 3,

$$f \approx \frac{\epsilon_{\max} \Delta\nu_{\frac{1}{2}}}{2.5 * 10^8} \quad \text{Equation (3)}$$

where $\Delta\nu_{1/2}$ is the width of the absorption band in wavenumbers at $\epsilon_{1/2}$ [58].

Because oscillator strength is based on molar extinction, a relatively high f is desired for a good optical limiter. For variations of TPP, oscillator strength values for the Soret band between 1.00 and 2.00 have been reported while the $Q_x(0-0)$ band has values in the 10^{-3} range [56, 59].

FLUORESCENCE

Another important optical property is fluorescence. Figure 18 shows a diagram of fluorescence and phosphorescence. The molecule absorbs a photon which causes an electronic excitation. This excess energy can be released through fluorescence, phosphorescence or nonradiative decay (heat). In Figure 18, fluorescence is shown as the drop from the S_1 state to the S_0 state. This is an allowed conversion with a rate constant of k_f . T_1 to S_0 is phosphorescence. In order for T_1 to be populated so that phosphorescence can occur, intersystem crossing from S_1 to T_1 is necessary. The rate constant for intersystem crossing is k_{ST} . The reverse, T_1 to S_1 and then a decay from S_1 to S_0 , is delayed fluorescence. The wavy lines in Figure 18 denote radiationless transfers. Chemical reaction and interaction with other molecules in solution are also possible ways to get rid of the excess energy. However, when low concentrations are used those pathways are minimized.

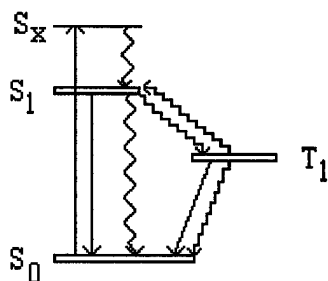


Figure 18. Absorption/Emission Basics

For optical limiting, fluorescence should be minimized. When fluorescence is significant, intersystem crossing is inefficient which decreases the population of the triplet state. Because population of the triplet state is what makes a good RSA optical limiter, strong fluorescence tends to indicate poor optical limiting performance.

QUANTUM YIELD

The quantum yield, ϕ , is the ratio between the number of photons emitted and the number of photons absorbed for the compound. For nonlinear absorption, a low fluorescence quantum yield, ϕ_f , is desired. With low fluorescence there is efficient intersystem crossing. This allows quantum yield for triplet formation, ϕ_t , to be maximized.

One method of measuring quantum yield is by relating the compound with an unknown quantum yield to a compound with a known quantum yield. For this method, equation 4 is used.

$$Q_u = Q_r \left(\frac{A_r(\lambda_r)}{A_u(\lambda_u)} \right) \left(\frac{I(\lambda_r)}{I(\lambda_u)} \right) \left(\frac{n_u^2}{n_r^2} \right) \left(\frac{D_u}{D_r} \right) \quad \text{Equation (4)}$$

where Q is the quantum yield, $A(\lambda)$ is the absorbance/cm of the solution at the exciting wavelength λ , $I(\lambda)$ is the relative intensity of the exciting light at wavelength λ , n is the

average refractive index of the solution, and D is the integrated area under the emission spectrum. The subscript u refers to the unknown solution while the subscript r refers to the reference solution [60]. In order to simplify the calculation, the UV-VIS spectra of both the reference and unknown can be used to find crossover points, points in which both the reference and the unknown have the same absorption at the same wavelength. The concentration of the reference is varied so that the crossover occurs at an absorption around 0.1 and near the maxima of the peaks. Doing this makes $A(\lambda)$ the same for both reference and unknown. Because one instrument is run at the same wavelength for the reference and unknown solutions within a short period of time, $I(\lambda)$ are the same for the reference and unknown solutions because instrument drift is not an issue. This reduces equation 4 to equation 5.

$$Q_u = Q_r \left(\frac{n_u^2}{n_r^2} \right) \left(\frac{D_u}{D_r} \right) \quad \text{Equation (5)}$$

Equation 5 requires certain assumptions in order to be valid [60]. The integrated luminescence intensity must be proportional to the fraction of light absorbed. With high optical densities, luminescence is sometimes only on the front surface of the cuvette which makes the proportion nonlinear. To avoid this problem, a maximum absorption of approximately 0.1 is used to make sure the solutions have low optical densities. Other assumptions needed are that all geometrical factors must be identical, the excitation beams must be monochromatic, the reflection losses need to be the same, internal reflection effects need to be equal, reabsorption and reemission need to be negligible, all light emanating from the cuvette must be isotropic, and the slit widths need to be the same.

This method was used by Loppnow *et al* with much success in the study of porphyrins [61].

Quantum yield can also be understood through equations. Equation 6 is a more theoretical definition of quantum yield of emission,

$$\Phi_e = \Phi_* k_e^0 \tau \quad \text{Equation (6)}$$

where Φ_* is the formation efficiency of the emitting state, k_e^0 is the rate constant for emission, and τ is the measured experimental lifetime of the emitting state [58]. The definition of experimental lifetime, τ , is shown in equation 7,

$$\tau \equiv \frac{1}{k_e^0 + \sum k_i} \quad \text{Equation (7)}$$

where $\sum k_i$ is the sum of all rate constants that deactivate the emitting state [58]. Because the emitting state is the absorbing state, Φ_* is unity, $k_e = k_f$, and $\sum k_i = k_{ST}$ [58]. Thus, equation 6 reduces to equation 8.

$$\Phi_f = k_f \tau_s = \frac{k_f}{k_f + k_{ST}} \quad \text{Equation (8)}$$

To minimize Φ_f , either k_f needs to be very small or k_{ST} needs to be very large.

HAMMETT SIGMA

For this project, a quantitative method for comparison of the electron donating/withdrawing properties of the substituent groups was desired so that changes in the optical properties caused by those groups could be compared more accurately. This problem was resolved with the use of the Hammett sigma parameter. The Hammett σ is a sum of both resonance and field effects of a group attached to a benzene ring. In 1991,

Hansch *et al* compiled a list of all examples where both σ_m and σ_p were reported [62].

When multiple values existed in the prior literature, they selected the set that seemed most reliable. These values have been determined using the Hammett equation shown in equation 9, organic reactions, or ^{19}F NMR substituent chemical shifts [62].

$$\sigma_x = \log K_X - \log K_H \quad \text{Equation (9)}$$

In this equation, K_H is the ionization constant for benzoic acid in water at 25 °C and K_X is the constant for the substituted benzoic acid. Values exist for the *para* and *meta* positions [62]. This treatment usually fails for the *ortho* position, thus no *ortho* values are available. An electron withdrawing group has a positive σ while an electron donating group has a negative σ value.

In 1975, Meot-Ner and Adler reported using the Hammett sigma to study substituent-induced frequency shifts of the porphyrins they studied, including some *para* substituted TPP. They found that, for free base spectrum shifts, the best correlation was given by the combination σ coefficient equation, $a_R\sigma_R + a_I\sigma_I$ [53]. This equation splits the resonance and field effects so that the percentage of each contributing to the change can be determined. The values for a_R and a_I are the respective percentages due to resonance and field effects, and they total unity when added together. The σ_R and σ_I are the resonance and field components of σ_p . This is shown in equation 10.

$$\sigma_R + \sigma_I = \sigma_p \quad \text{Equation (10)}^{62}$$

Meot-Ner and Adler determined that when $a_R = 0.8$ and $a_I = 0.2$, their data showed the best correlation [53]. Such a high amount of resonance was unusual because the phenyl rings are not in the plane of the porphyrin skeleton, due to steric hindrance.

STERIC HINDRANCE

While the Hammett σ works well for *meta* and *para* substituents, steric hindrance is where *ortho* substituents have their greatest effect. When the phenyl rings are added to the basic porphyrin skeleton, the rings cannot remain coplanar with the skeleton. This is shown in Figure 19.

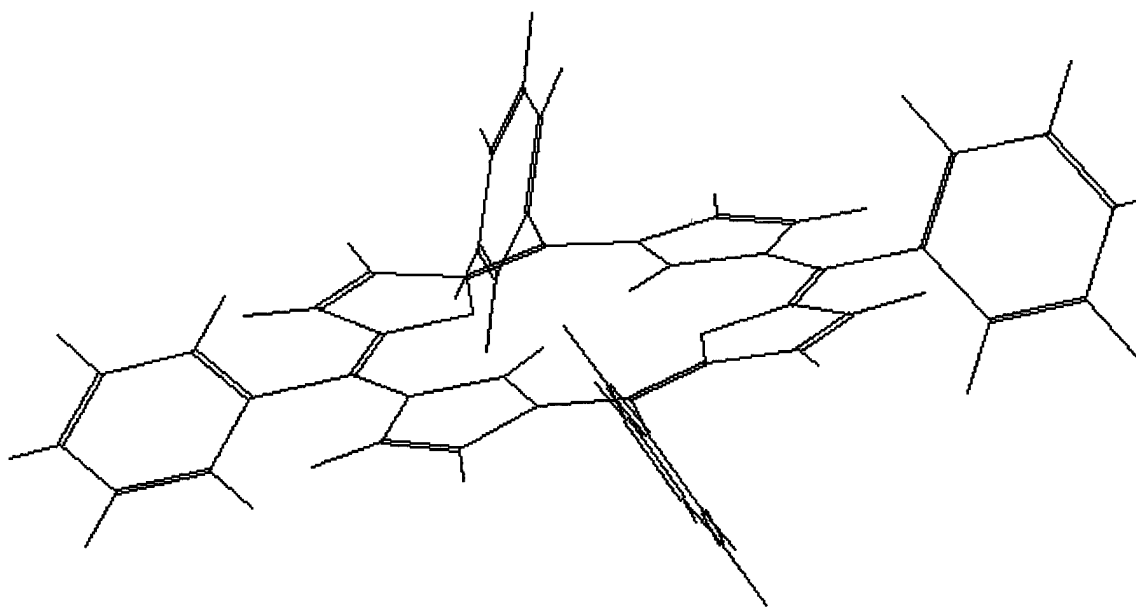


Figure 19. Energy Minimized Structure of TPP⁶³

According to Meot-Ner and Adler, there are approximately 40 degrees between the phenyl and porphyrin planes for TPP in solution [53]. Adding a substituent to the *ortho* position of the phenyl groups creates steric problems. As the phenyl group rotates, the *ortho* substituent sterically interacts with the porphyrin π system [64, 65]. This steric repulsion causes a decrease in the energy of orbital b_1 . An *ortho* effect for TPP has been reported before [53, 56, 64]. These researchers all found a blue shift in the absorption for

substituents in the *ortho* position when compared to the absorption of the same substituent in the *para* position. The decrease in energy of orbital b_1 results in an increase in the energy of the transition, thus giving a blue shift.

Even though the porphyrin nucleus and the phenyl groups are not coplanar, Meot Ner and Adler showed that resonance interactions are still significant [53]. The phenyl rings interact conjugatively and inductively with orbital b_1 because of the nodal properties of orbitals b_1 and b_2 [64].

BASIC STATISTICS

When a large number of points are available, it is easy to see if a real trend exists. Because of the small sample size, statistical tests were necessary to be sure the general trend seen was statistically significant. Two tests were used, R^2 and the F test statistic.

R is the multiple correlation coefficient. The value of R^2 tells the proportion of variability in y explained by y 's relationship with x [66]. Its maximum is 1 which indicates a perfect correlation while its minimum value of 0 indicates no correlation. One problem is that high correlation coefficients can be obtained in models with no physical meaning [67]. To make sure there is meaning in the fit, the F test statistic is used.

The F test statistic is a test for a lack of fit. It is used to compare the variance from two normal populations [66]. The F distribution is used in conjunction with the F test statistic to determine the confidence interval. For most experiments, a 95% confidence is sufficient [68]. Thus, as long as the confidence given by the F statistic is at least 95%, there is a trend.

PURPOSE

Thus, the purpose of this research was to study optical properties of various substituted tetraphenyl porphyrins. The basic TPP structure, shown in Figure 2 and 13, was modified by adding substituent groups to the attached phenyl rings and monitoring their effect on UV-VIS absorption, molar extinction coefficient, oscillator strength, fluorescence emission, and fluorescence quantum yield. The specific optical properties studied can be used to predict the optical limiting capability of the compounds.

This process adds to the expanding knowledge of porphyrins so that, some day in the future, dyes can be more easily designed for specific sensors as needed. The electron donating/withdrawing capacity of the modified groups on the porphyrin can also be used to help design dyes. Using Hammett sigma plots, comparisons were made to the UV-VIS maximum absorption, molar extinction coefficient, oscillator strength, fluorescence emission and fluorescence quantum yield. Trends in these optical properties are influenced by the electron donating/withdrawing groups which affect the conjugated π -electron system. These trends clearly show that substituents can enhance or detract from the optical limiting performance of a dye, thus leading to the evolution of more promising materials.

II. EXPERIMENTAL

COMPOUNDS USED

All compounds were obtained from Dr. Weijie Su at MLPJ, Air Force Research Laboratory, Wright Patterson Air Force Base. The basic TPP molecule, shown in Figures 2 and 19, was modified by adding substituents to the phenyl rings. Table 1 shows the phenyl rings with the added substituents. It also shows the solvent used for molar extinction and quantum yield.

The Hammett σ values used are shown in Table 2. The σ_m is only listed for those compounds that have a *meta* substituent on the phenyl ring. The σ_p listed is for the *para* substituent. The σ_R and σ_I are listed for those compounds with only a *para* substituent.

Table 1. Substituents Added


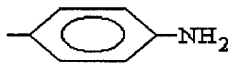
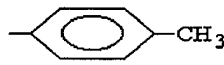



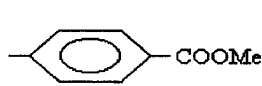
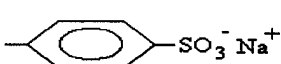
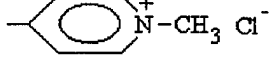
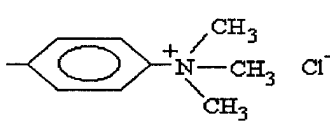
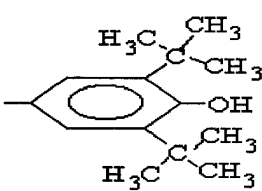
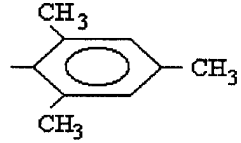
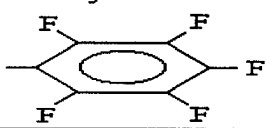
Compound (Other Abbreviation)	Solvent	R ₁ , R ₂ , R ₃ , R ₄
TPP	toluene	
TNH ₂ PP	DCM	
TCH ₃ PP	DCM	
TOCH ₃ PP	DCM	
TOHPP	MeOH	
TCOOHPP	DMF	
TCOOMePP	DCM	
TSO ₃ NaPP	H ₂ O	
TMePyP	H ₂ O	
T(CH ₃) ₃ NPP (Cl)	H ₂ O/MeOH	
T 3,5-di-t-butyl-4-hydroxy PP (Tt-butylOHPP)	DMF/DCM	
T Mesityl PP	DMF/DCM	
TPFPP	DMF/DCM	

Table 2. Hammett Sigma Values

Compound	σ_m	σ_p	Total σ	σ_R	σ_I
TNH ₂ PP		-0.66	-0.66	0.08	-0.74
T t-butylOH PP	-0.10	-0.37	-0.57		
TOHPP		-0.37	-0.37	0.33	-0.70
TOCH ₃ PP		-0.27	-0.27	0.29	-0.56
T Mesityl PP		-0.17	-0.17		
TCH ₃ PP		-0.17	-0.17	0.01	-0.18
TSO ₃ PP		0.35	0.35	0.29	0.06
TCOOHPP		0.45	0.45	0.34	0.11
TCOOMePP		0.45	0.45	0.34	0.11
TPFPP	0.34	0.06	0.74		
T(CH ₃) ₃ NPPCl		0.82	0.82	0.86	-0.04

ABSORPTION λ_{\max} SHIFT STUDY

A Perkin Elmer Lambda 9 UV/VIS/NIR Spectrophotometer was used to obtain the UV-VIS absorption spectra of each compound from 300nm to 800nm. Quartz cells were used for all measurements. To prevent skewing from solvent effects, the same solvent was used for all the compounds to determine λ_{\max} shifting due to substituent groups. This could be done because concentration and intensity of absorption were not an issue. The solvent used was a mix of equal parts DCM, DMF, and MeOH. The λ_{\max} of each peak was then compared for all the compounds.

MOLAR EXTINCTION COEFFICIENT

The Perkin Elmer Lambda 9 UV/VIS/NIR Spectrophotometer was used to obtain the UV-VIS absorption spectrum of each compound from 300nm to 800nm. Due to the concentrations that were necessary for the calculation, different solvents were used based on the compound and are shown above in Table 1. A series of nine known concentrations

was made for each compound. Beers Law and linear regression were then used to calculate molar extinction coefficient for each peak in the absorption spectrum observed for each compound.

OSCILLATOR STRENGTH

The molar extinction coefficient and the corresponding UV-VIS absorption spectrum were used to calculate oscillator strength with equation 3.

FLUORESCENCE SHIFT STUDY

A Perkin Elmer Luminescence Spectrometer LS 50B was used to measure the fluorescence emission of each compound. To prevent skewing from solvent effects, the same solvent was used for all the compounds to determine the fluorescence spectral shifting due to substituents. The solvent used was equal parts DCM, DMF, and MeOH. The peak fluorescence emission wavelength for each compound was then compared.

QUANTUM YIELD DETERMINATION

The Lambda 9 and the LS 50B were used to determine the quantum yield for each compound. The Lambda 9 was used to determine crossover points in the UV-VIS spectrum for the sample and a standard with a known quantum yield. TPP in toluene was used as the standard. It has a known quantum yield of 0.1 [69]. The concentration of TPP was varied so that the crossover occurred at an absorption of around 0.1 and so that the crossover took place near the maxima of the peak. The wavelength of the crossover was then used as the excitation wavelength on the LS 50B. The emission slit, excitation slit, and scan speed were constant for all the spectra obtained. The scan range and number of scans was kept constant for each sample/standard pair of spectra. The scan range was

made wide enough so that the baseline was as close to zero as possible on both sides of the peak in order to minimize error. The area of the fluorescence spectrum was then calculated by the computer. The quantum yield was calculated using equation 5. The average refractive index of the solutions were found using CRC [70]. Multiple measurements with different crossover points were completed for each compound and the results were averaged to increase accuracy. The samples were in the same solvents used for the molar extinction calculation.

III. RESULTS & DISCUSSION

PORPHYRIN ABSORPTION SPECTRA

The different substituent groups added to the phenyl rings of TPP produced changes in the relative intensities of the Q bands. A sample Q band spectrum for each compound is in Appendix A. The relative intensities of the peaks are shown in Table 3 and can be explained with Gouterman's model. For ease in reading the table $Q_x(0-0)$ is labeled 1, $Q_x(0-1)$ is 2, $Q_y(0-0)$ is 3, and $Q_y(0-1)$ is 4.

Table 3. Relative Q Band Intensities

Compound	Relative Band Intensities
TNH ₂ PP	$3 > 4 > 1 > 2$
Tt-butylOHPP	$3 \geq 4 > 1 > 2$
TOHPP	$4 > 3 > 1 > 2$
TOCH ₃ PP	$4 \gg 3 > 1 > 2$
TMesitylPP	$4 \gg 3 \geq 2 > 1$
TCH ₃ PP	$4 \gg 3 > 2 \geq 1$
TPP	$4 \gg 3 > 2 \geq 1$
TSO ₃ NaPP	$4 \gg 3 \geq 2 > 1$
TCOOHPP	$4 \gg 3 > 2 > 1$
TCOOMePP	$4 \gg 3 > 2 > 1$
TPFPP	$4 \gg 2 \gg 1$
T(CH ₃) ₃ NPP (Cl)	$4 \gg 3 \geq 2 > 1$
TMePyP	$4 \gg 2 > 3 \gg 1$

Starting with the free base porphyrin, Gouterman found that Figure 10 A was true.

Adding the four phenyl groups adds electron density to orbital b_1 raising it in relation to orbital b_2 . Electron donating groups increase the energy of orbital b_1 further while

electron withdrawing groups decrease orbital b_1 . Raising the energy of orbital b_1 causes a larger relative difference between the transitions for Q_x and Q_y which causes their respective (0-0) peaks to gain strength. This is why the Q_x (0-0) and Q_y (0-0) bands increase in relative strength as more electron donating groups are added.

As seen above, the Q_x (0-0) and Q_y (0-0) transitions are affected more than the Q_x (0-1) and Q_y (0-1) transitions. This is because the vibronic interaction removes some of the forbidden nature of the (0-1) transitions. Since the (0-0) bands are still forbidden, they start off weak and show large variation. The (0-1) bands, with some of the forbiddenness removed, are relatively stable in intensity.

ABSORPTION λ_{\max} SHIFTING

Table 4 shows the results of the peak shifts.

Table 4. Absorption Peak Shifts

Compound	Soret Band (nm)	Q_y (0-1) (nm)	Q_y (0-0) (nm)	Q_x (0-1) (nm)	Q_x (0-0) (nm)
TNH ₂ PP	432	525	569	594	661
Tt-butylOHPP	423	521	560	596	653
TOHPP	422	518	556	594	651
TOCH ₃ PP	423	517	554	593	650
TMesitylPP	418	512	544	589	646
TCH ₃ PP	418	514	550	590	646
TPP	417	513	548	588	645
TSO ₃ NaPP	418	513	548	589	644
TCOOHPP	417	514	549	589	645
TCOOMePP	418	513	548	589	644
TPFPP	415	504		580	653
T(CH ₃) ₃ NPP (Cl)	416	512	546	587	646
TMePyP	426	516	552	590	646

To make sure solvent interaction differences in the peak shift were minimized, the same mixed solvent was used for all the compounds. Electron donating groups tended to give a red shift compared to TPP while electron withdrawing groups have little effect. Electron donating groups increase the electron density of orbital b_1 thus increasing the energy of the orbital. This leads to a decrease in the energy of the transition, thus the red shift. Both Hammett σ and the combination σ coefficient equation were used to quantify this trend. Wavenumbers (cm^{-1}) were used to improve accuracy as well. The results for the Soret and Q_x (0-0) bands compared to σ are shown in Figures 20 and 21. The same bands were compared to the combined σ coefficient equation value and are shown in Figures 22 and 23.

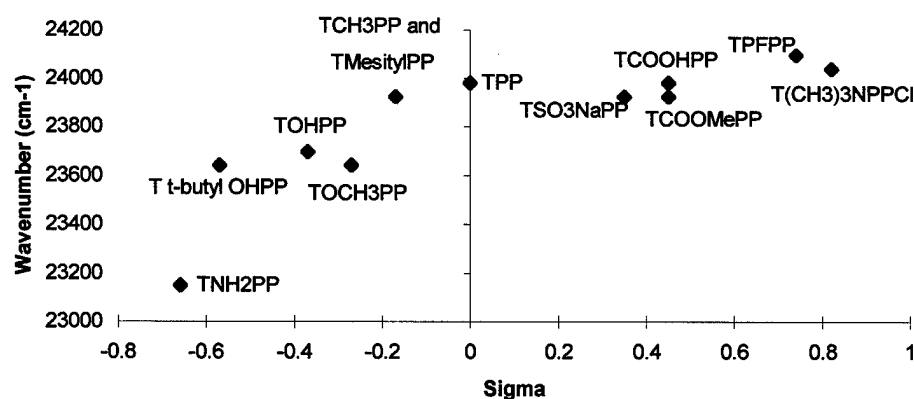


Figure 20. Absorption λ_{max} Shift versus Hammett σ : Soret Band

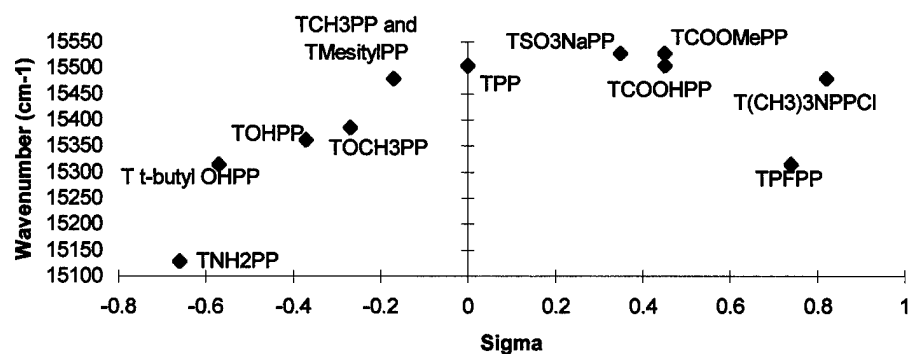


Figure 21. Absorption λ_{\max} Shift versus Hammett σ : Q_x (0-0) Band

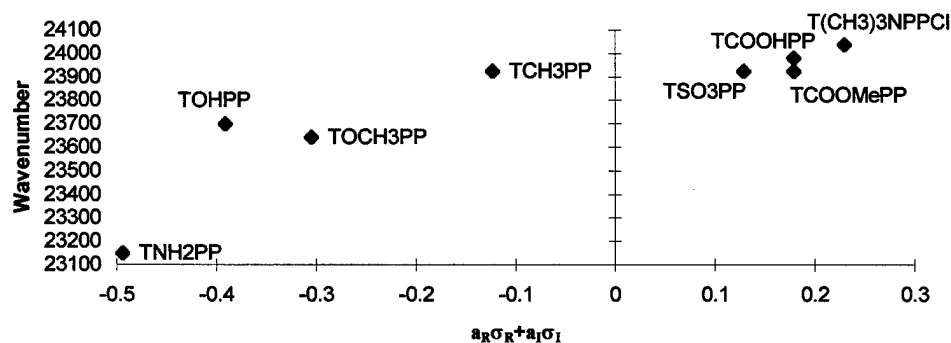


Figure 22. Absorption λ_{\max} Shift versus Combined σ : Soret Band

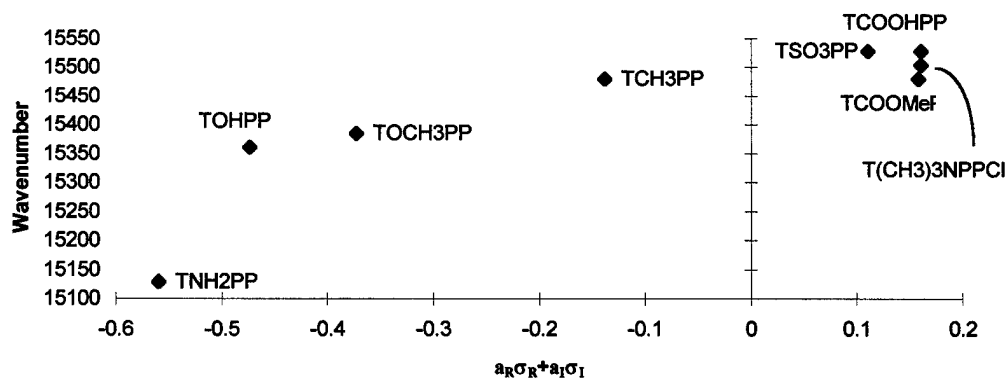


Figure 23. Absorption λ_{\max} Shift versus Combined σ : Q_x (0-0) Band

All the bands show a correlation between electron donating/withdrawing strength and the absorption λ_{max} . For Figure 20, the R^2 is 0.80 and the F statistic corresponds to a 99.92% confidence. With Figure 21, the R^2 is 0.81 and the F statistic corresponds to a 99.94% confidence. The correlation is improved after TMesitylPP and TPFPP are removed, especially for $Q_x(0-0)$. The R^2 for $Q_x(0-0)$ increases to 0.92 and the F statistic corresponds to 99.99% confidence with those compounds removed. This improvement is due to that fact that the Hammett σ is not accurate for substituents in the *ortho* position of the phenyl rings. The difference seen in shifting is because of steric repulsion of the electrons in orbital b_1 . This leads to a decrease in the energy of orbital b_1 which results in an increase in the energy of transition. Thus, there is a blue shift in the actual peak seen compared to what would be expected from a compound with that Hammett σ .

For the combined σ coefficient plots, Figures 22 and 23 show the combined σ with the coefficient values that give the best fit. For Figure 22, $a_R = 0.7$ and $a_I = 0.3$ while Figure 23 has an $a_R = 0.78$ and an $a_I = 0.22$. This shows that resonance is the main method of interaction between the added substituents and the porphyrin nucleus, but that inductance does occur and is important. While the overall result that resonance is largest is the same, this coefficient for resonance is slightly lower than the $a_R = 0.8$ reported by Meot-Ner and Adler [53]. The differences seen could be due to solvent effects.

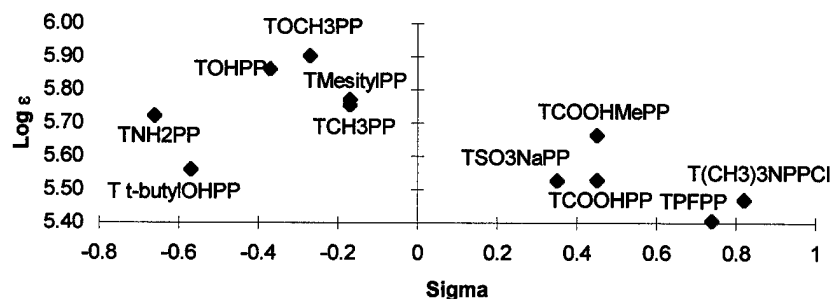
MOLAR EXTINCTION COEFFICIENT

The calculated log molar extinction coefficient values are shown in Table 5.

Table 5. Molar Extinction Coefficient

Compound	Soret Band log ϵ	Q_y (0-1) log ϵ	Q_y (0-0) log ϵ	Q_x (0-1) log ϵ	Q_x (0-0) log ϵ
TNH ₂ PP	5.72	4.06	4.10	3.67	3.81
Tt-butylOHPP	5.56	4.26	4.27	3.90	3.99
TOHPP	5.86	4.10	3.99	3.63	3.68
TOCH ₃ PP	5.90	4.27	4.10	3.75	3.88
TMesitylPP	5.77	4.29	4.76	3.73	3.52
TCH ₃ PP	5.75	4.27	4.02	3.64	3.68
TPP [57]	5.62	4.22	3.95	3.70	3.60
TSO ₃ NaPP	5.53	4.12	3.74	3.68	3.45
TCOOHPP	5.53	4.20	3.88	3.75	3.64
TCOOMePP	5.66	4.32	3.98	3.76	3.61
TPFPP	5.40	4.30		3.84	3.41
T(CH ₃) ₃ NPP (Cl)	5.47	4.16	3.74	3.74	3.46
TMePyP	5.27	4.14	3.69	3.76	3.15

In order to see if there was a trend in the strength of ϵ based on electron donating/withdrawing strength, the Hammett σ and the combined σ coefficient were used. These values were plotted against log ϵ . The results for the Soret and Q_x (0-0) bands for the Hammett σ are shown in Figures 24 and 25. The same bands were compared to the combined σ coefficient equation and the best coefficient value plot for each are shown in Figures 26 and 27.

Figure 24. Soret Band Molar Extinction Coefficient versus Hammett σ

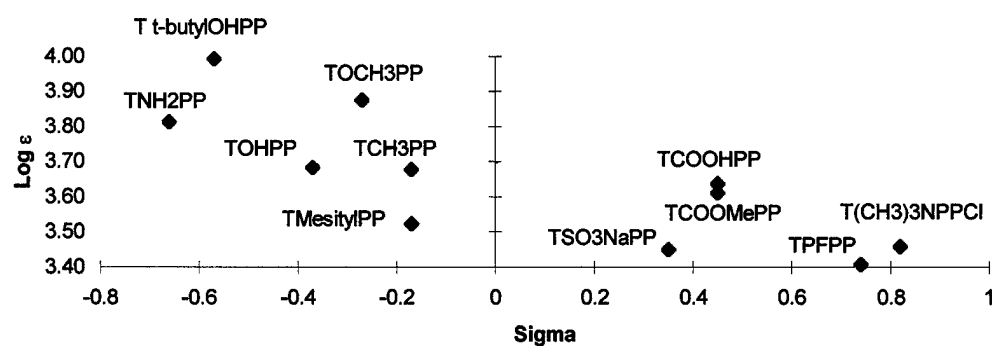


Figure 25. Q_x (0-0) Band Molar Extinction Coefficient versus Hammett σ

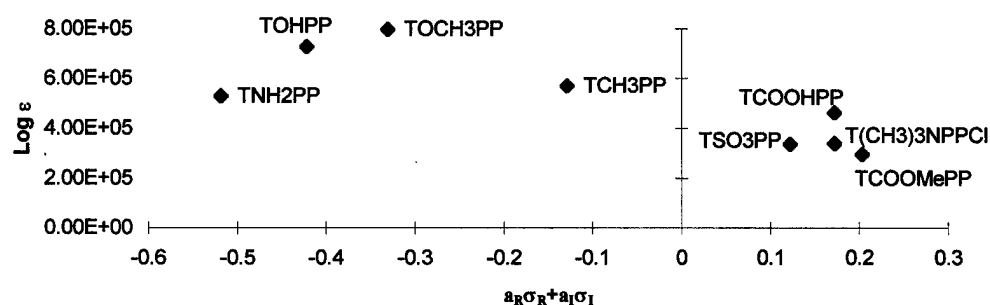


Figure 26. Soret Band Molar Extinction Coefficient versus Combined σ

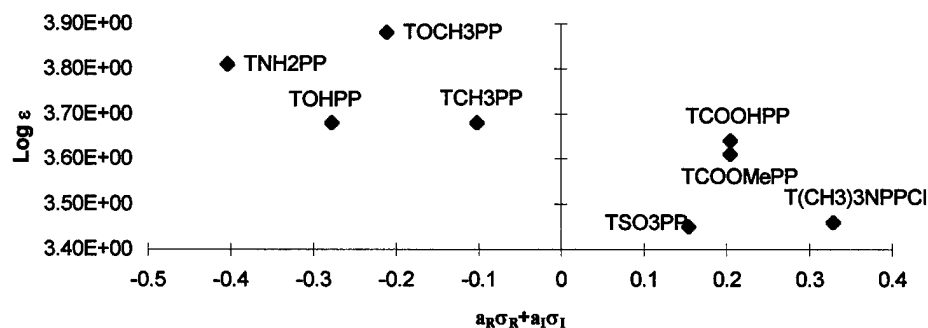


Figure 27. Q_x (0-0) Band Molar Extinction Coefficient versus Combined σ

As shown in the graphs, there is a correlation between $\log \epsilon$ and electron donating/withdrawing strength. According to the F test, these correlations are significant, however the R^2 values are not as impressive. For Figure 24, the R^2 is only 0.67 and the F statistic corresponds to 98.75% confidence. The R^2 for Figure 25 is only 0.66 and the F test shows a 98.68% confidence. This is probably because of solvent effects. Because exact concentration was needed for the calculation of molar extinction over a wide range of concentrations, different solvents were used. Molar extinction is solvent dependent, which would skew the correlation enough to lower the R^2 value.

For the $Q_x(0-0)$ band, the fit is improved by dropping TMesitylPP. This changes the R^2 to 0.75 and the F test gives a 99.19% confidence. Again, this is probably because of the *ortho* methyl groups steric interactions with orbital b_1 .

With the combined σ coefficient plots, only the best fit for the coefficients are shown. For Figure 26, $a_R = 0.73$ and $a_I = 0.27$ while Figure 27 has an $a_R = 0.59$ and an $a_I = 0.41$. Again, resonance is the main method of interaction but inductance does occur and is important.

A large molar extinction coefficient is desired for a better dye. Based on that fact and the values determined, more electron donating groups improve the molar extinction coefficient. Thus, adding an electron donating group to a dye with a poorer molar extinction coefficient could improve its value.

OSCILLATOR STRENGTH

Oscillator strength was calculated using equation 3 and the values are reported in Table 6.

Table 6. Calculated Oscillator Strength

Compound	Soret Band f
TNH ₂ PP	2.13
Tt-butylOHPP	2.46
TOHPP	2.23
TOCH ₃ PP	1.50
TMesitylPP	1.30
TCH ₃ PP	1.81
TSO ₃ NaPP	1.18
TCOOHPP	0.88
TCOOMePP	1.39
TPFPP	1.30
T(CH ₃) ₃ NPP (Cl)	0.98
TMePyP	1.08

The Hammett σ and the combined σ coefficient were used to compare these results based on electron donating/withdrawing capacity. These can be seen in Figures 28 and 29, respectively.

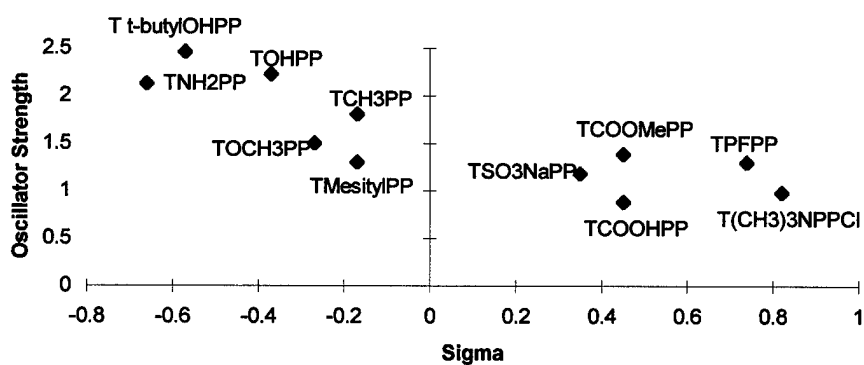


Figure 28. Oscillator Strength versus Hammett σ

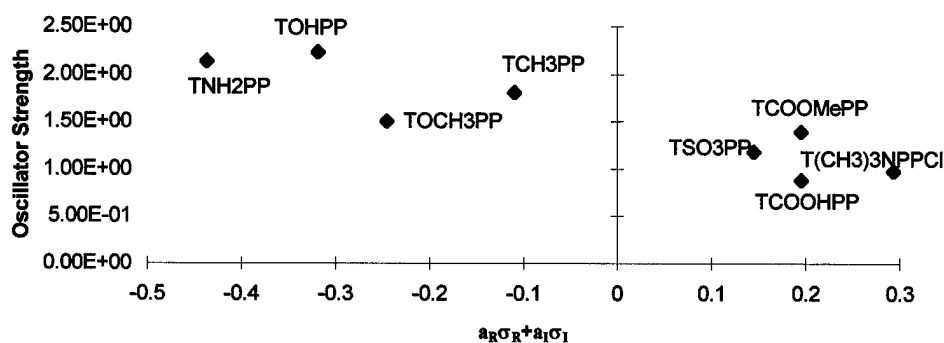


Figure 29. Oscillator Strength versus Combined σ

A trend towards lower oscillator strength as the substituents become more electron withdrawing is seen. This follows the same trend as ϵ , which was expected based on equation 3. However, these oscillator strength values contain much error. There is error due to solvent effects and error due to the approximate nature of the calculation. Thus these values only show the trend and are probably not the exact oscillator strengths. The R^2 for this is 0.77 and the F test statistic shows a 99.7% confidence. Dropping TMesitylPP and TPFPP improves the R^2 to 0.83 while the F test statistic remains virtually unchanged at 99.5%.

For Figure 29, the $a_R = 0.65$ and the $a_I = 0.35$. Again, resonance was stronger of the two but inductance was important.

Because of its relationship to molar extinction coefficient, oscillator strength should also be relatively high for a better dye. Based on these calculations, more electron donating groups improve the value of oscillator strength.

FLUORESCENCE SPECTRA SHIFTING

Fluorescence spectra shifts followed the same trend as the absorption spectra shifts. The wavelength for the fluorescence peak for each sample is shown in Table 7. A sample fluorescence spectrum for each compound studied is in Appendix B.

Table 7. Fluorescence Peak Shifts

Compound	Fluorescence shift
TNH ₂ PP	678
Tt-butylOHPP	664
TOHPP	662
TOCH ₃ PP	659
TMesitylPP	650
TCH ₃ PP	654
TPP	651
TSO ₃ NaPP	651
TCOOHPP	652
TCOOMePP	651
TPFPP	640
T(CH ₃) ₃ NPP (Cl)	650
TMePyP	656

As shown in Figure 30, electron donating groups gave a red shift while electron withdrawing groups give a blue shift.

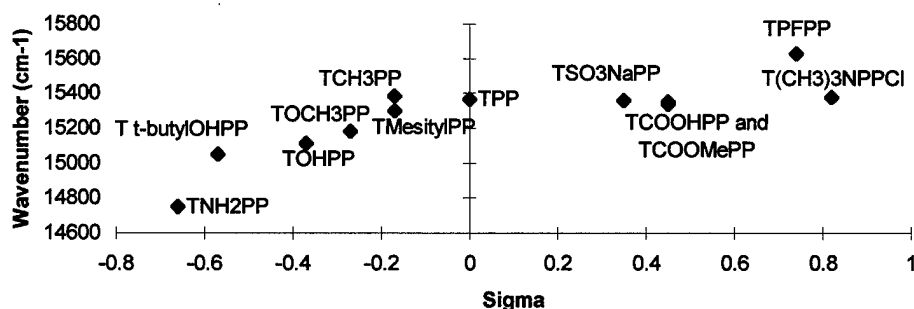


Figure 30. Fluorescence versus Hammett σ

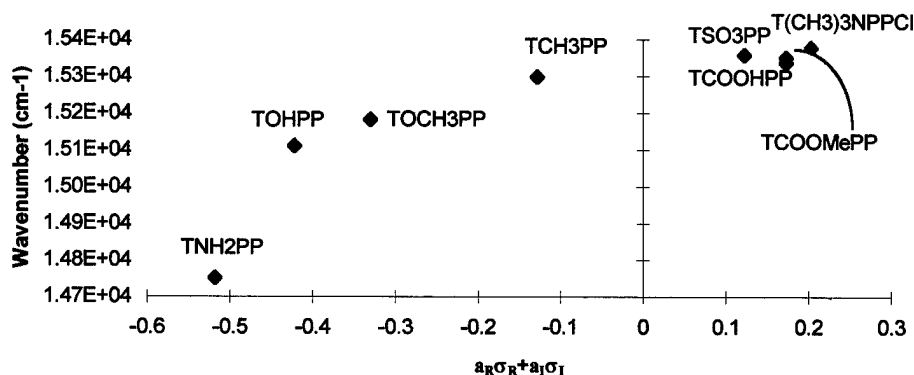


Figure 31. Fluorescence versus Combined σ

The trend seen is clearer than that of ϵ and f because a mixed solvent was used to minimize skewing from solvent effects. For Figure 30, the R^2 is 0.79 and the F statistic gives a confidence of 99.91%. An improvement is seen when TMesitylPP and TPFPP are removed. The R^2 increases to 0.89 and the F statistic gives a confidence of 99.96%.

Figure 31 shows the best combined σ coefficient for the fluorescence peak shifting, where $a_R = 0.73$ and $a_I = 0.27$. As expected, these values are very similar to the a_R and a_I values for the absorption λ_{\max} shifting.

For optical limiting, fluorescence peak shifting is not very important. However, in finding the fluorescence peak shift, the strength of the fluorescence can be seen. All of these compounds had strong fluorescence which indicates poor intersystem crossing. Thus, this specific group of compounds will probably not show very good optical limiting.

QUANTUM YIELD

The fluorescence quantum yield was calculated using equation 5. Table 8 shows the solvent corrected ϕ_f values calculated.

Table 8. Fluorescence Quantum Yield

Compound	ϕ_f
TNH ₂ PP	0.137
Tt-butylOHPP	0.132
TOHPP	0.107
TOCH ₃ PP	0.122
TMesitylPP	0.095
TCH ₃ PP	0.103
TPP [69]	0.100
TSO ₃ NaPP	0.109
TCOOHPP	0.072
TCOOMePP	0.088
TPFPP	0.075
T(CH ₃) ₃ NPP (Cl)	0.075
TMePyP	0.035

Again, Hammett σ and the combined σ were used to compare the results. These graphs can be seen in Figures 32 and 33.

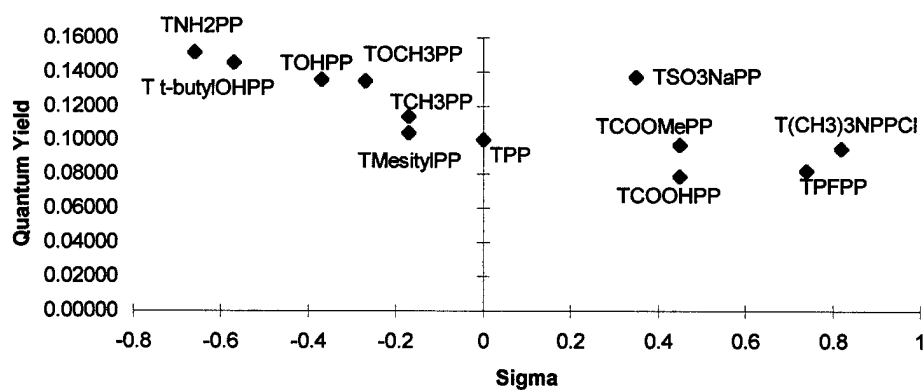


Figure 32. Quantum Yield versus Hammett σ

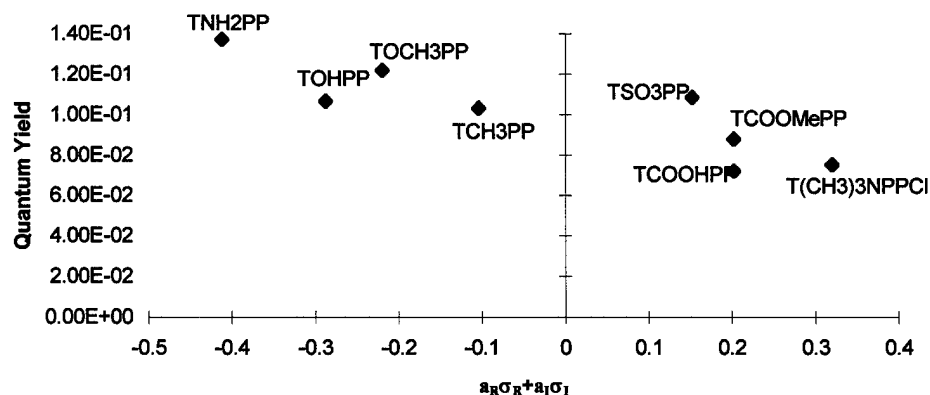


Figure 33. Quantum Yield versus Combined σ

As seen in both graphs, electron donating groups tended to have higher ϕ_f . The greater electron density causes an increase in the energy of orbital b_1 which decreases the energy of the transition. This makes it easier for electrons to be excited into higher states which increases the probability of photons being emitted. Using equation 8, k_f is probably large while k_{ST} is probably small.

For Figure 32, the R^2 is 0.66 while the F statistic gives a 99.23% confidence. Even though different solvents were used, corrections for the solvents were in the calculation itself. This kept solvent effects from skewing the values calculated.

With Figure 33, $a_R = 0.6$ while $a_I = 0.4$. This is a bit lower than values seen for a_R and a_I . This could be due to solvent effects. Even though the refractive index for the solvents are used in the calculation, the refractive index of each solvent was taken from CRC and was not determined for each solvent on the day they were used.

IV. CONCLUSION

The purpose of this project was to study the optical properties of TPP after various substituent groups were added to the phenyl rings. The electron donating/withdrawing capacity of those groups was used to determine if there were trends in the changes of the optical property being studied. These optical properties included UV-VIS absorption λ_{max} , molar extinction coefficient, oscillator strength, fluorescence shifting, and fluorescence quantum yield. The Hammett σ was used to quantify the electron donating/withdrawing nature of the substituted groups.

All the optical properties studied had a general inclination to increase or decrease in value based on the electron donating/withdrawing strength of the substituted groups. UV-VIS absorption λ_{max} had a red shift for more electron donating groups. Molar extinction coefficient and oscillator strength both showed an increase for electron donating groups. Fluorescence also showed a red shift with electron donating groups. Finally, fluorescence quantum yield showed an increase with electron donating groups.

The Hammett sigma was also split into its resonance and inductive components. Then the combined sigma equation was used to determine the extent of resonance in the molecule. An average of 69% resonance and 31% inductance was found, with a resonance high of 78% and low of 59%. This shows that, while resonance was the

strongest influence on the shifting of the optical properties, inductive effects did occur and were important.

The trends found in this study are important for the development of future dyes. In developing a dye, many compromises are necessary. While a substituted group might improve the performance of one optical property, it could decrease the performance of another. Besides being used to determine the optimum substituent group to add to improve a specific property, plots like the ones created could be used to determine how the other properties will most likely be affected and which property is most affected. For this series of compounds, besides the absorption λ_{max} shifting involved, fluorescence quantum yield had the most notable change based on the substituent group added. Thus, the best improvements for this group of compounds would involve focusing on decreasing the fluorescence quantum yield.

There are many future studies that could be completed. Future work on the specific molecules studied could include fluorescence lifetime determination, and time resolved fluorescence as well as actual laser tests. Fluorescence lifetime shows how long it takes before the compound in question emits energy. Time resolved fluorescence shows possible isomerization based on the shape of the curve obtained. Laser testing determines if optical limiting is actually occurring.

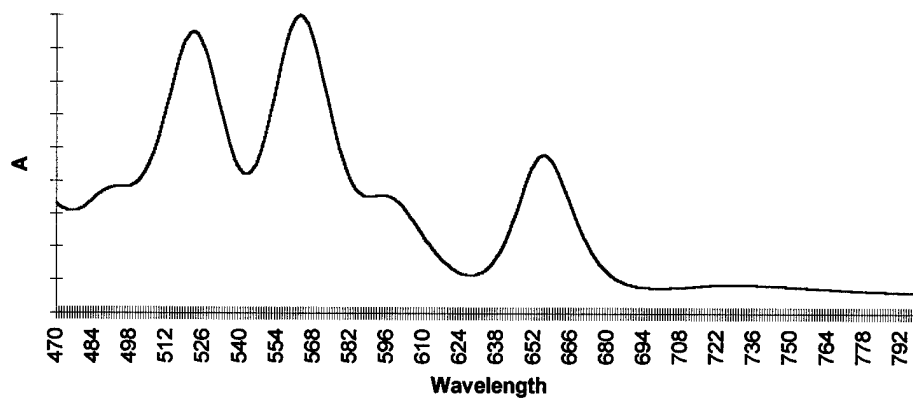
Another direction would be to study the addition of a metal to the compounds. Creating the metal salt tends to improve the optical limiting properties of the molecule. This is due to the heavy atom effect. A metal in the center of the porphyrin contributes small electronic and spin orbit perturbations. While the electronic perturbations cause

small differences in the absorption of the molecule, the spin orbit perturbations cause large changes in ϕ_f and ϕ_t [44]. Using Figure 1, the radiationless decay from S_1 to T_1 increases when a heavy atom is present. This populates the triplet state more and allows more phosphorescence to occur. Using equation 8, heavy metals increase the rate of intersystem crossing, k_{ST} , decreasing ϕ_f . Common metals used include cobalt, copper, and zinc.

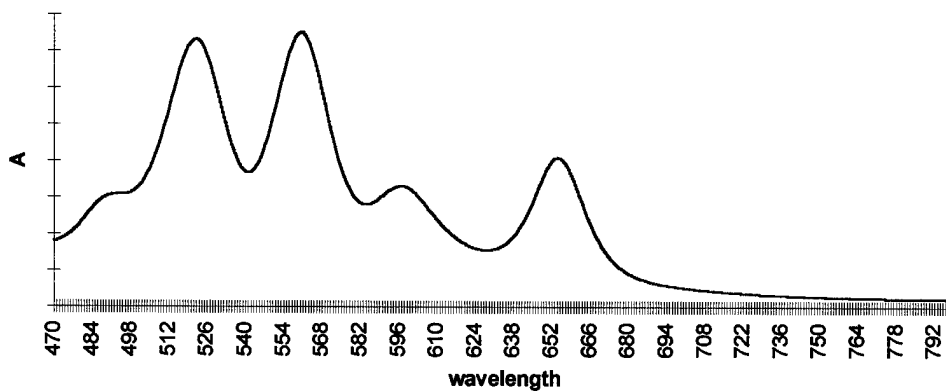
In conclusion, while this specific set of compounds do not appear to be very good optical limiting dyes, the trends in the changes in the optical properties reported can be used to help design both better dyes and future studies.

APPENDIX A

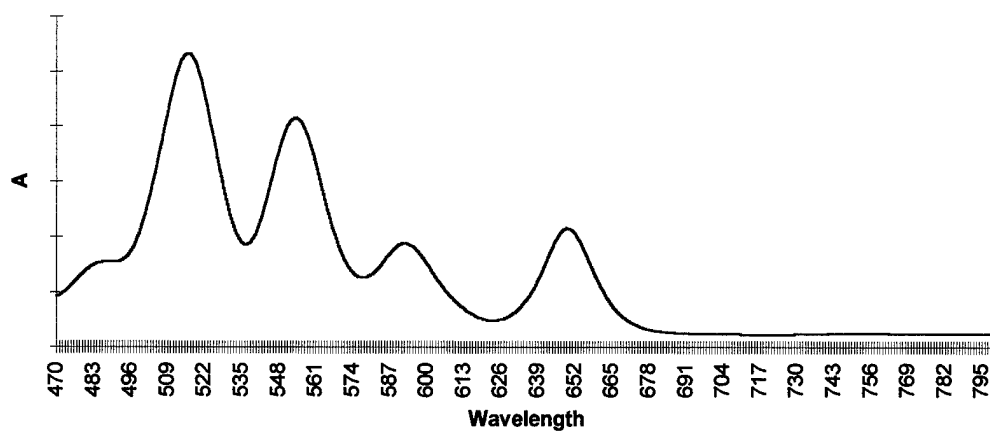
Sample Q band Absorption



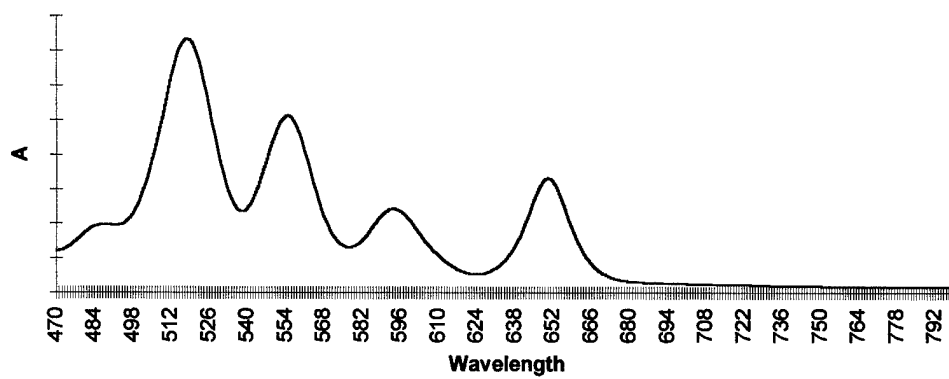
TNH₂PP



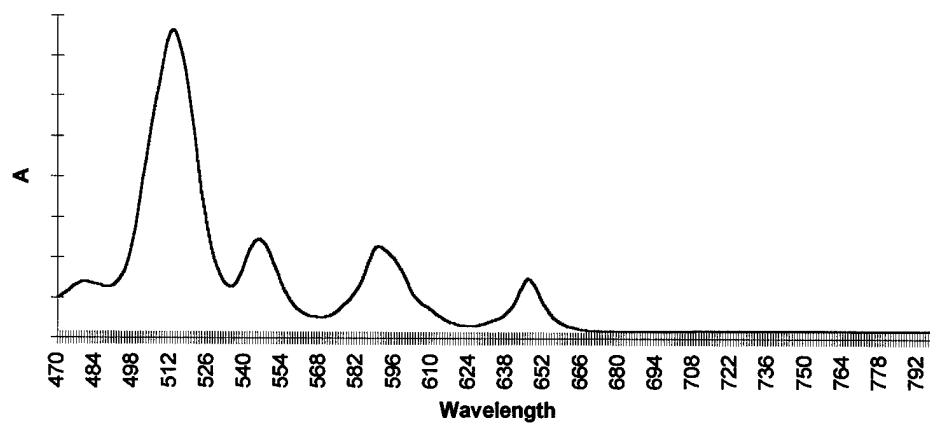
T 3,5-di-t-butyl-4-hydroxy PP



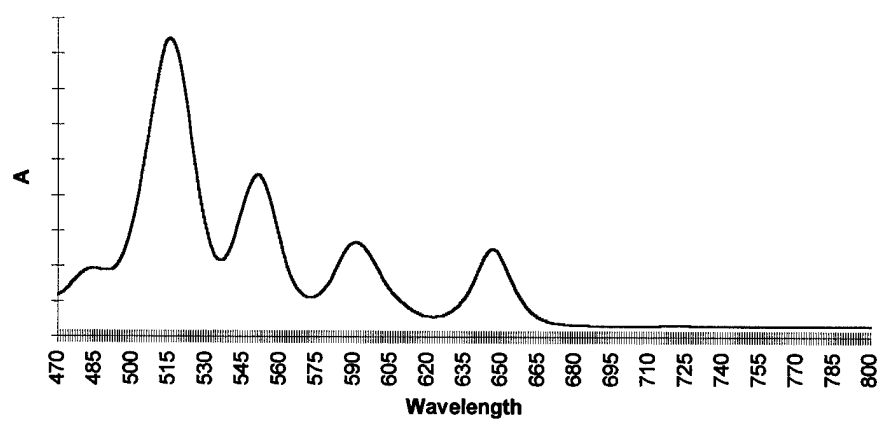
TOHPP



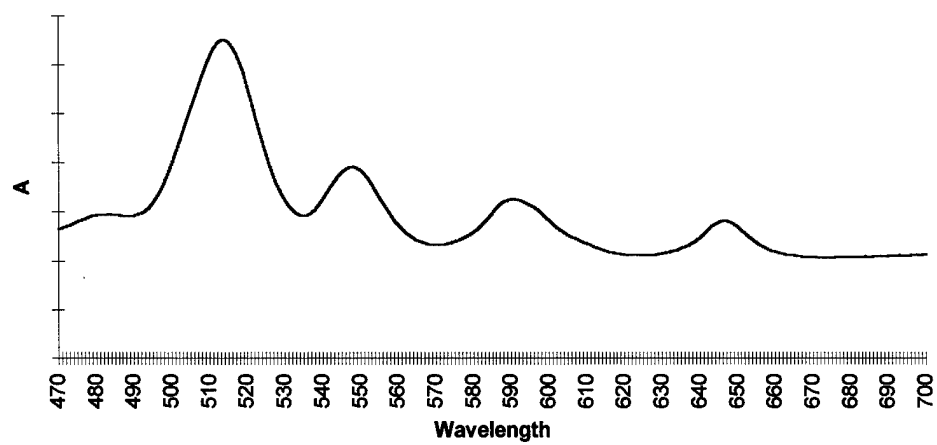
TOCH₃PP



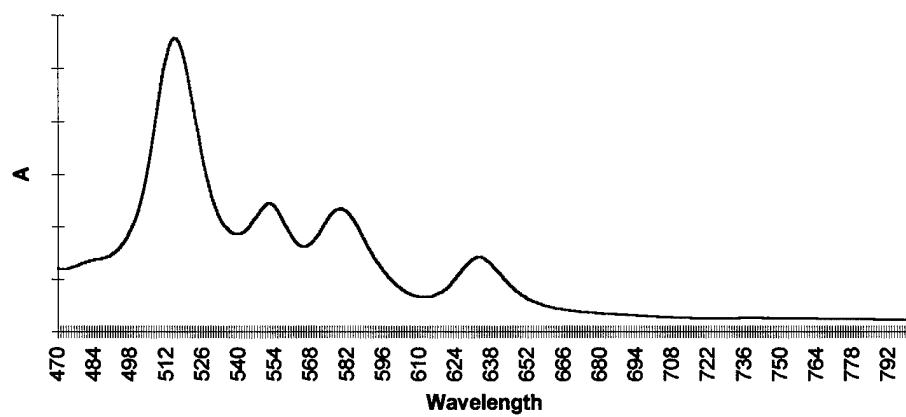
TMesitylPP



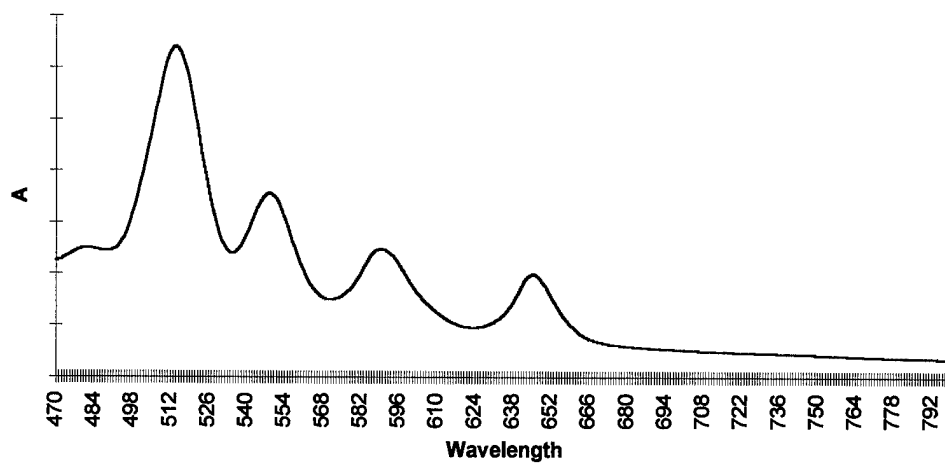
TCH₃PP



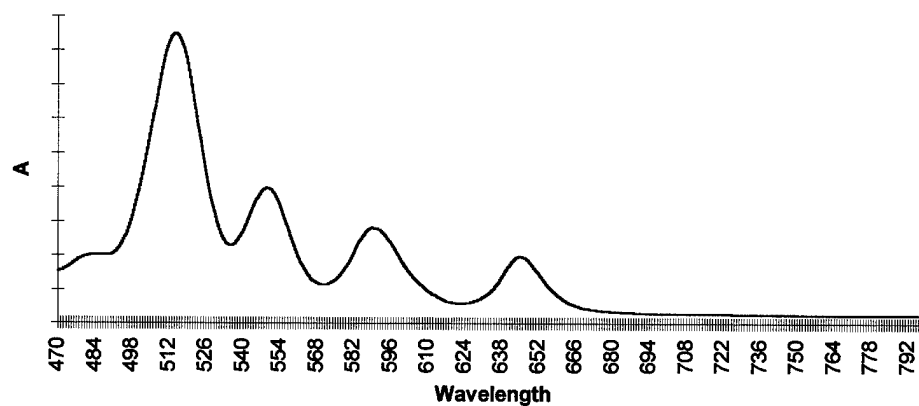
TPP



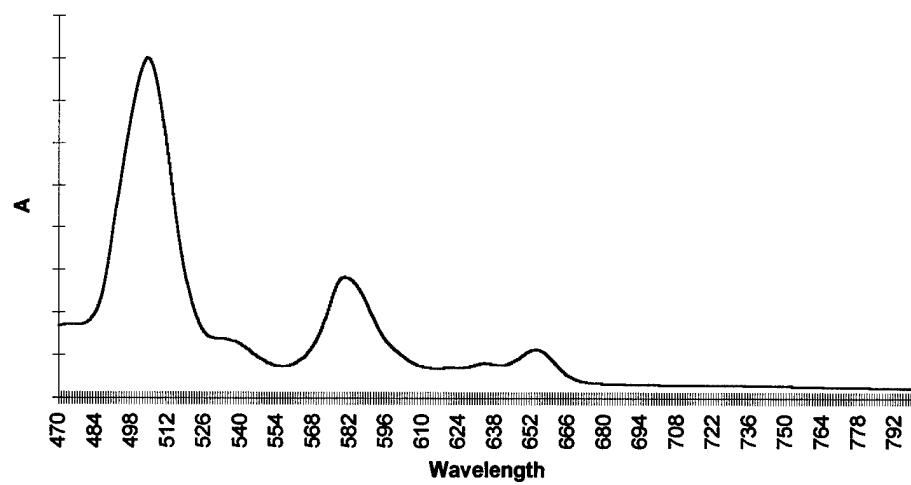
TSO₃NaPP



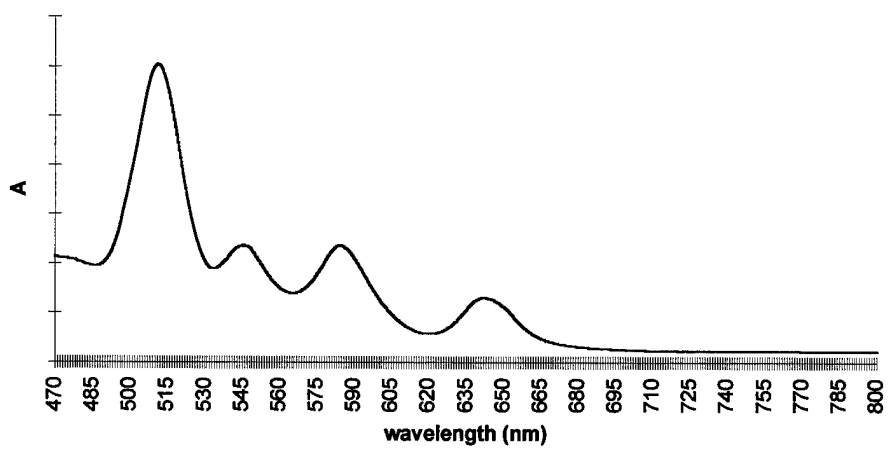
TCOOHPP



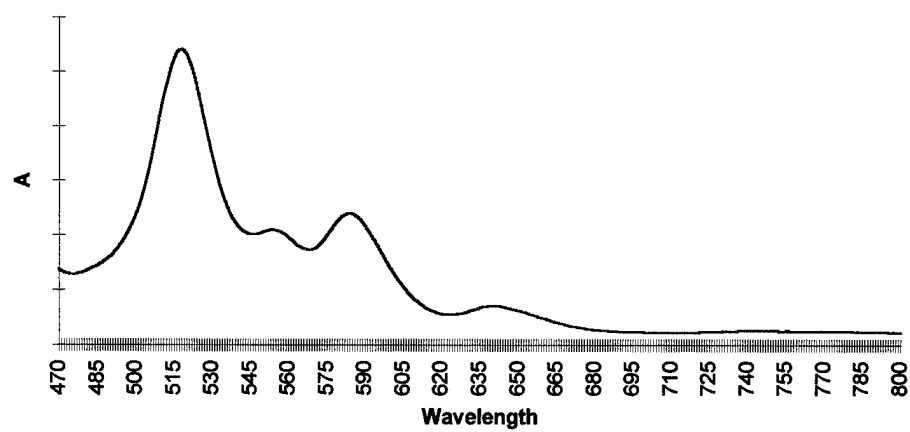
TCOOMePP



TPFPP



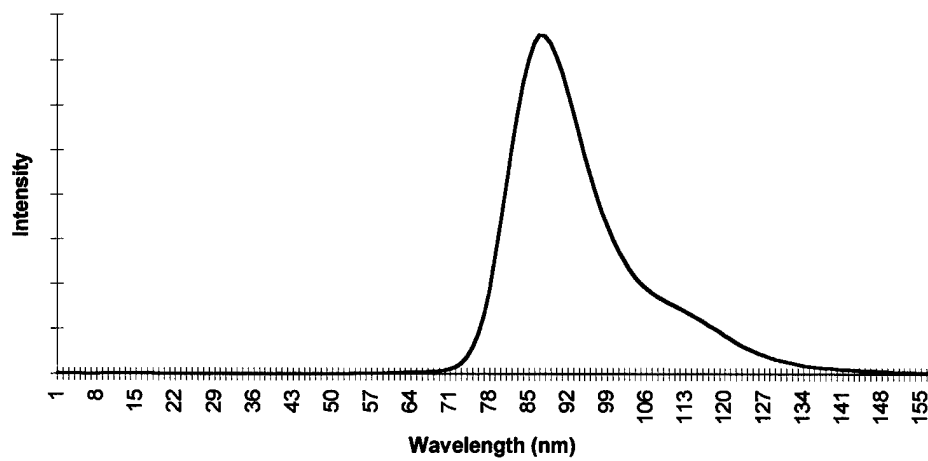
T(CH₃)₃NPP (Cl)



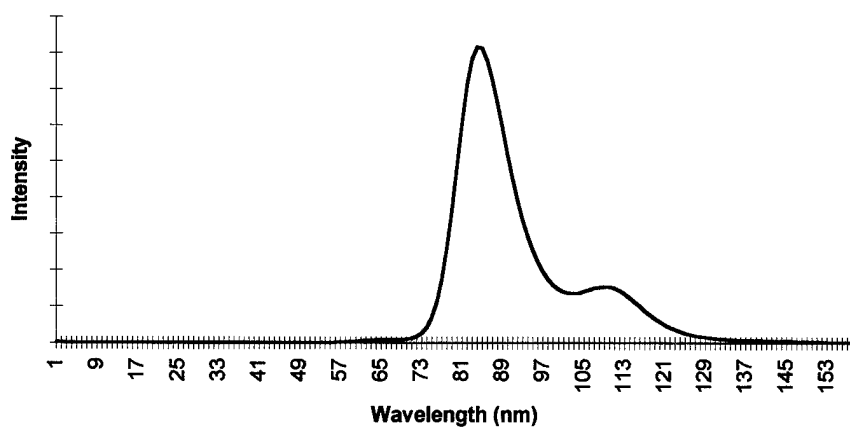
TMePyP

APPENDIX B

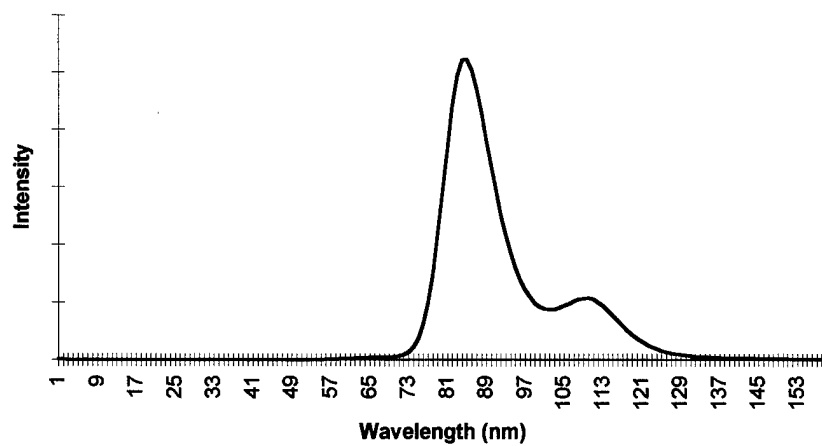
Sample Fluorescence Spectra



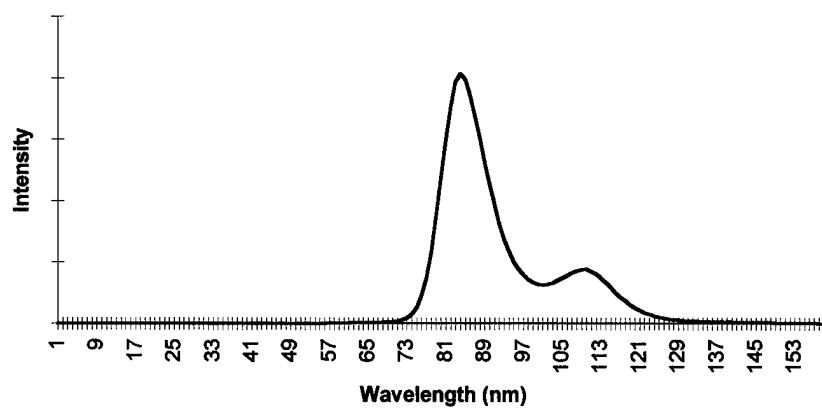
TNH₂PP



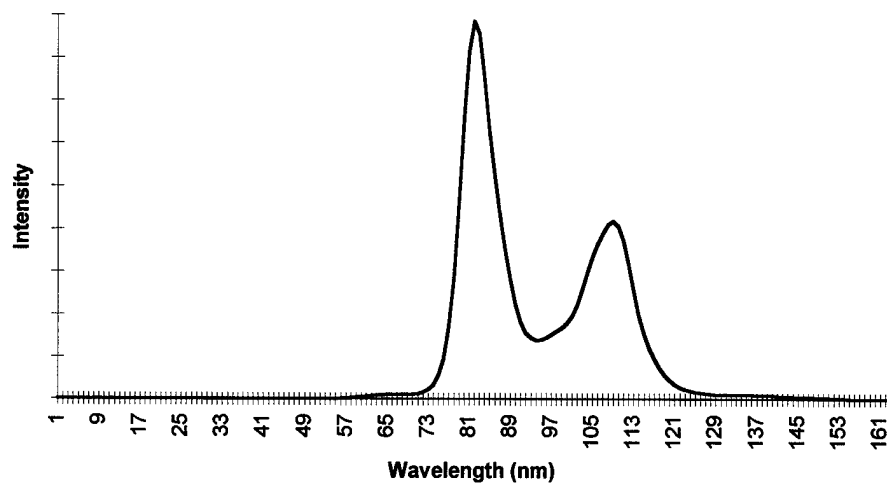
T 3,5-di-t-butyl-4-hydroxy PP



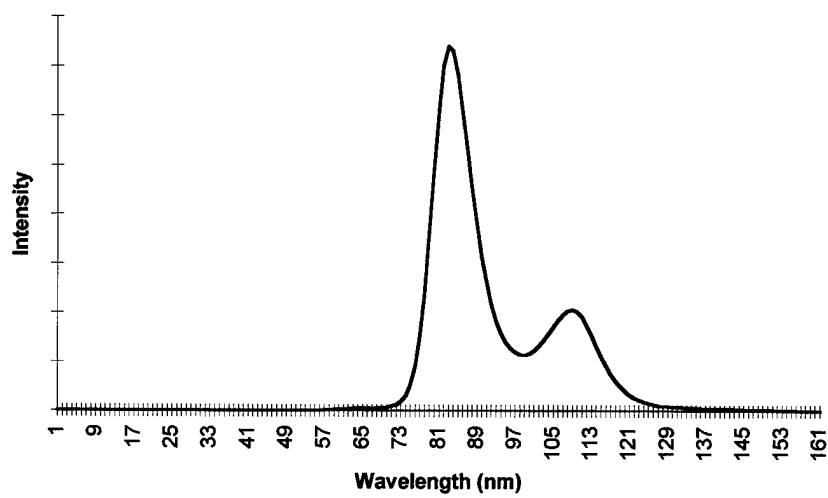
TOHPP



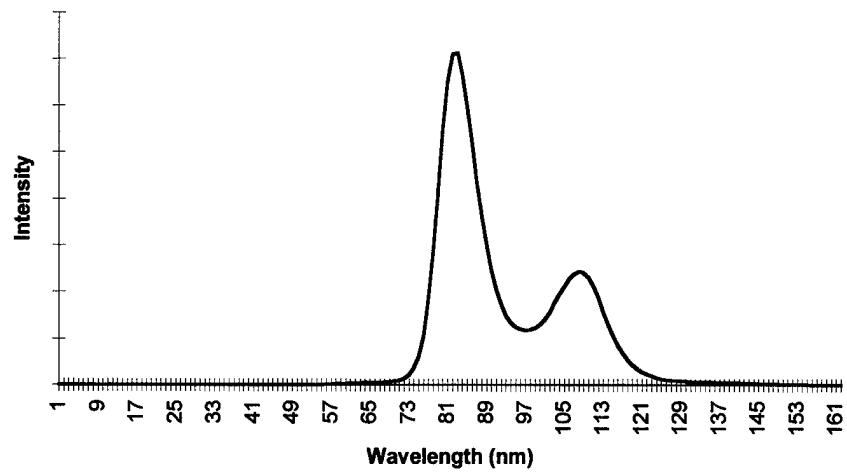
TOCH₃PP



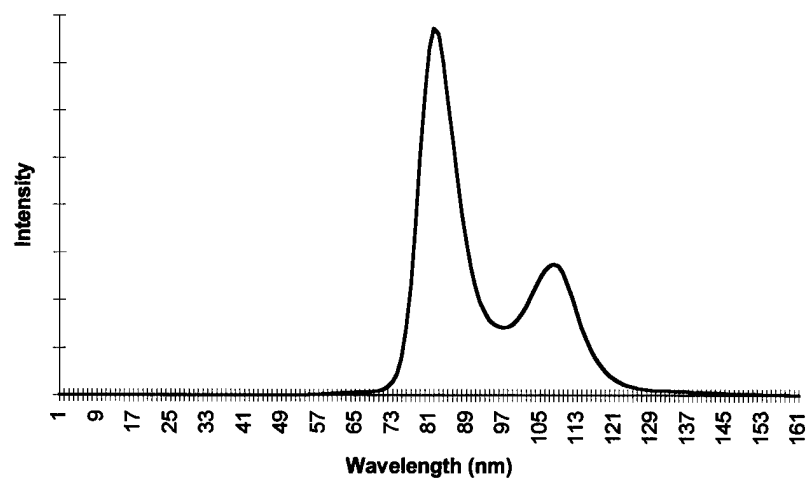
TMesitylPP



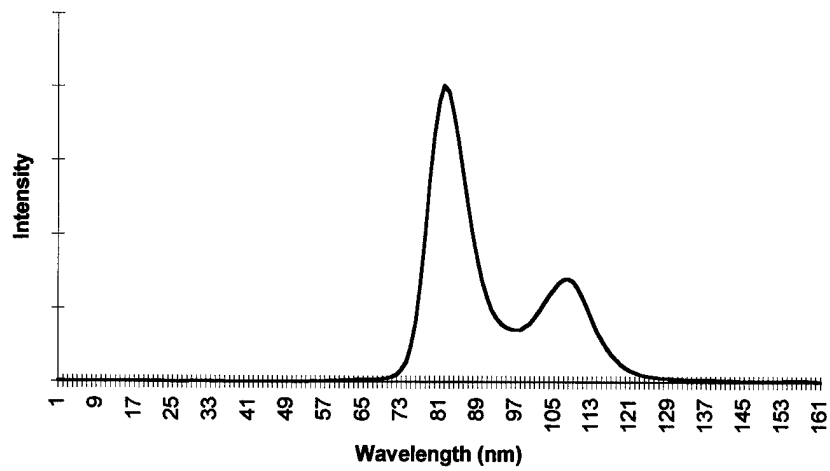
TCH₃PP



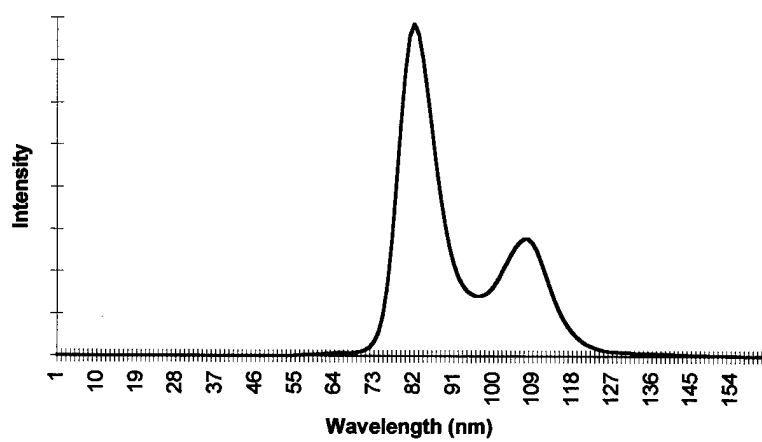
TPP



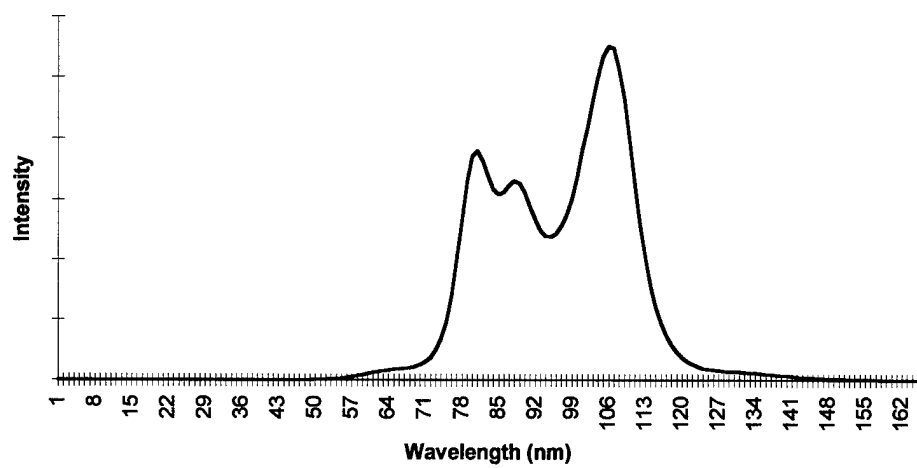
TSO₃NaPP



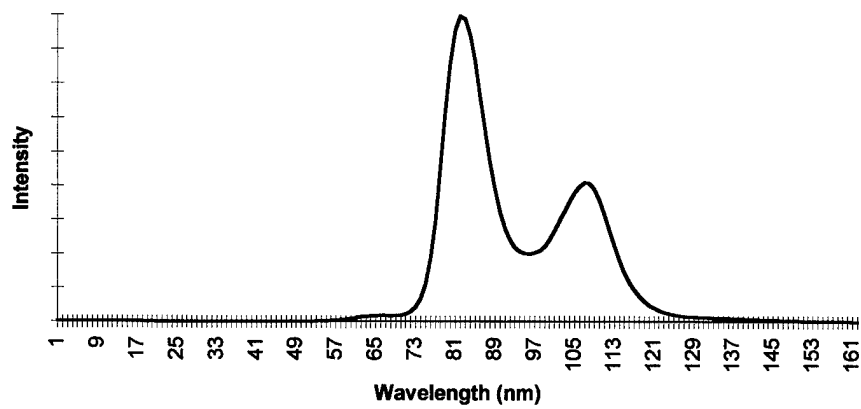
TCOOHPP



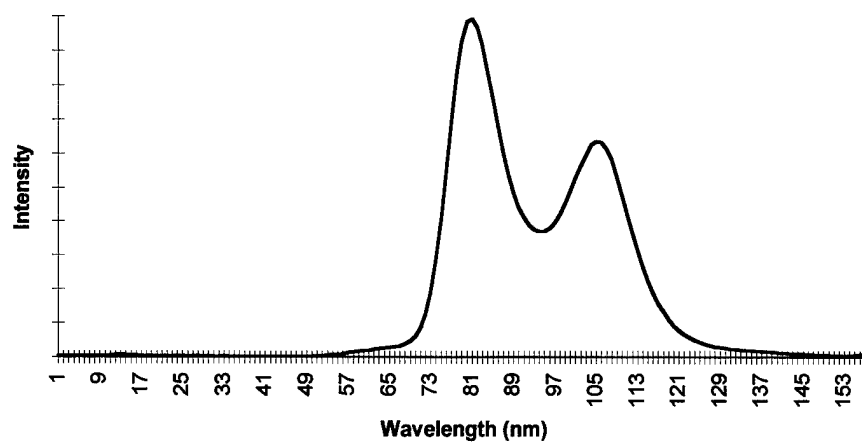
TCOOMePP



TPFPP



T(CH₃)₃NPP (Cl)



TMePyP

REFERENCES

- 1) L. W. Tutt and T. F. Boggess. *Prog. Quant. Electr.* **17**, 299-338 (1993).
- 2) W. Su, T. M. Cooper, and M. C. Brant. *Chem. Mater.* **10**, 1212-1213 (1998).
- 3) T. J. Bunning, L.V. Natarajan, M. G. Schmitt, B. L. Epling, and R. L. Crane. *Appl. Opt.* **30**, 4341 (1991).
- 4) A. C. Walker, A. K. Kar, Ji Wei, U. Keller, and S. D. Smith. *Appl. Phys. Lett.* **48**, 683 (1986).
- 5) Yia Chung Chang, A. E. Chiou and M. Khoshnevisan. *J. Appl. Phys.* **71**, 1349 (1992).
- 6) G. L. Woods, W. W. Clark, M. J. Miller, G. J. Salamo, and E. J. Sharp. *Materials for Optical Switches, Isolators, and Limiters.* **1105**, 154 (1989).
- 7) J. Kleinschmidt, S. Rentsch, W. Tottleben, and B. Wilhelmi. *Chem. Phys. Lett.* **24**, 133 (1974).
- 8) J. L. Oudar. *Chem. Phys.* **67**, 446 (1977).
- 9) P. A. Fleitz, R. L. Sutherland, L. V. Natarajan, T. Pottenger, and N. C. Fernelius. *Opt. Lett.* **17**, 716 (1992).
- 10) R. J. M. Anderson, G. R. Holtom and W. M. McClain. *J. Chem. Phys.* **70**, 4310 (1979).

- 11) L. V. Natarajan, L. A. Sowards, C. W. Spangler, N. Tang, P. A. Fleitz, R. L. Sutherland, and T. M. Cooper. *Mat. Res. Soc. Symp. Proc.* **479**, 135 (1997).
- 12) R. L. Swofford and W. M. McClain. *J. Chem. Phys.* **59**, 5740 (1973).
- 13) J. A. Bennett and R. R. Birge. *J. Chem. Phys.* **73**, 4234 (1980).
- 14) R. L. Sutherland, E. Rea, L. V. Natarajan, T. Pottenger, and P. A. Fleitz. *J. Chem. Phys.* **98**, 2593 (1993).
- 15) L. V. Natarajan, R. L. Sutherland, M. G. Schmitt, M. C. Brant, and D. G. McLean. *Proc. SPIE.* **1853**, 99 (1993).
- 16) C. R. Guiliano and L. D. Hess. *IEEE J. Quantum Electron.* **3**, 358 (1967).
- 17) L. V. Natarajan, R. L. Sutherland, D. McLean, M. Brant, D. M. Brandelik, T. M. Cooper, and R. L. Crane. *Mat. Res. Soc. Symp. Proc.* **374**, 231 (1995).
- 18) J. W. Arbogast, A. P. Darmanyan, C. S. Foote, Y. Rubin, F. N. Diederich, M. M. Alvarez, S. J. Anz, and R. L. Whetten. *J. Phys. Chem.* **95**, 11 (1991).
- 19) D. G. McLean, R. L. Sutherland, M. C. Brant, D. M. Brandelik, P. A. Fleitz, and T. Pottenger. *Opt. Lett.* **18**, 858 (1993).
- 20) L. W. Tutt and A. Kost. *Nature.* **356**, 225 (1992).
- 21) F. Henari, J. Callaghan, H. Stiel, W. Blau, and D. J. Cardin. *Chem. Phys. Lett.* **199**, 144 (1992).
- 22) F. Bentivegna, M. Canva, P. Georges, A. Brun, F. Chaput, L. Malier, and J. P. Boilot. *Appl. Phys. Lett.* **62**, 1721 (1993).
- 23) M. C. Brant, D. M. Brandelik, D. G. McLean, R. L. Sutherland, and P. A. Fleitz. *Mol. Cryst. Liq. Cryst.* **256**, 807 (1994).

- 24) D. Birnbaum, B. E. Kohler, and C. W. Spangler. *J. Chem. Phys.* **94**, 1684 (1991).
- 25) C. W. Spangler, P. K. Liu, A. A. Dembek, and K. O. Havelka. *J. Chem. Soc.* 799 (1991).
- 26) D. R. Coulter, V. M. Miskowski, J. W. Perry, T. H. Wei, E. W. Vanstryland, and D. J. Hagan. *Proc. SPIE.* **1105**, 42 (1989).
- 27) J. W. Perry, K. Mansour, S. R. Marder, K. J. Perry, D. Alvarez, and I. Choong. *Opt. Lett.* **19**, 625 (1994).
- 28) J. W. Perry, K. Mansour, I. Y. S. Lee, X. L. Wu, P. V. Bedworth, C. T. Chen, D. Ng, S. R. Marder, P. Miles, T. Wada, M. Tian, and H. Sasabe. *Science.* **273**, 1533 (1996).
- 29) W. Blau, H. Byrne, W. M. Dennis, and J. M. Kelly. *Opt. Comm.* **56**, 25 (1985).
- 30) R. Bonnett, A. Harriman, and A. N. Kozyrev. *J. Chem. Soc. Faraday Trans.* **88**, 763 (1992).
- 31) P. Bhyrappa, and V. Krishnan. *Inorg. Chem.* **30**, 239 (1991).
- 32) T. Takeuchi, H. B. Gray, and W. A. Goddard III. *J. Am. Chem. Soc.* **116**, 9730 (1994).
- 33) D. Mandon, P. Ochsenbein, J. Fischer, R. Weiss, K. Jayraj, R. N. Austin, A. Gold, P. S. White, O. Brigaud, P. Battioni, and D. Mansuy. *Inorg. Chem.* **31**, 2044 (1995).
- 34) E. R. Birnbaum, J. A. Hodge, M. W. Grinstaff, W. P. Schaefer, L. Henling, J. A. Labinger, J. E. Bercaw, and H. B. Gray. *Inorg. Chem.* **34**, 3625 (1995).

- 35) F. D. Souza, A. Villard, E. V. Caemelbecke, M. Franzen, T. Boschi, P. Tagliatesta, and K. M. Kadish. *Inorg. Chem.* **32**, 4042 (1993).
- 36) E. R. Birnbaum, W. P. Schaefer, J. A. Labinger, J. E. Bercaw, and H. B. Gray. *Inorg. Chem.* **34**, 1751 (1995).
- 37) J. A. Hodge, M. G. Hill, and H. B. Gray. *Inorg. Chem.* **34**, 809 (1995).
- 38) N. Tang, W. Su, T. Cooper, W. Adams, D. Brandelik, M. Brant, D. McLean, and R. Sutherland. *Proc. SPIE.* **2853**, 149 (1996).
- 39) N. Tang, W. Su, D. Krein, D. McLean, M. Brant, P. Fleitz, D. Brandelik, R. Sutherland, and T. Cooper. *MRS Proc.* **479**, (1997).
- 40) W. Su, T. Cooper, N. Tang, D. Krein, H. Jiang, D. Brandelik, P. Fleitz, M. Brant, and D. McLean. *MRS Proc.* **479**, 313 (1997).
- 41) M. Gouterman. *J. Mol. Spectrosc.* **6**, 138 (1961).
- 42) M. Perrin, M. Gouterman, and C. Perrin. *J. Chem Phys.* **50**, 4137 (1969).
- 43) M. Gouterman. *J. Chem. Phys.* **30**, 1139 (1959).
- 44) M. Gouterman, in D. Dolphin (ed.), *The Porphyrins*, Vol. III, Academic Press, New York, 1979, p 1-165.
- 45) V. Balke, F. A. Walker, and J. West. *J. Am. Chem. Soc.* **107**, 1226 (1985).
- 46) G. H. Barnett, M. F. Hudson, and K. M. Smith. *J. Chem. Soc. Perkin Trans.* **1**, 1401 (1975).
- 47) A. D. Adler, F. R. Longo, J. D. Finarelli, J. Goldmacher, J. Assour, and L. Korsakoff. *J. Org. Chem.* **32**, 476 (1967).

- 48) A. D. Adler, F. R. Longo, F. Kampas, and J. Kim. *J. Inorg. Nucl. Chem.* **32**, 2443 (1970).
- 49) J. Lindsey and R. Wagner. *J. Org. Chem.* **54**, 828 (1989).
- 50) File obtained from Dr. Weijie Su.
- 51) H. C. Longuet-Higgins, C. W. Rector, and J. R. Platt. *J. Chem. Phys.* **18**, 1174 (1950).
- 52) I. Chen. *J. Mol. Spectrosc.* **23**, 144 (1967).
- 53) M. Meot-Ner and A. Adler. *J. Am. Chem. Soc.* **97**, 5107 (1975).
- 54) J. Robinson. *Undergraduate Instrumental Analysis*. Marcel Dekker Inc, New York, 1995, p 263.
- 55) T. Gouw. *Guide to Modern Methods of Instrumental Analysis*, Wiley-Interscience, New York, 1972, p 162.
- 56) J. Kim, J. Leonard, and F. Longo. *J. Am. Chem. Soc.* **94**, 3986 (1972).
- 57) H. Anderson. *Tetrahedron Letters* **33**, 1101 (1992).
- 58) N. Turro. *Modern Molecular Photochemistry*. University Science Books, Sausalito, 1991.
- 59) P. Seybold and M. Gouterman. *J. Mol. Spectrosc.* **31**, 1 (1969).
- 60) J. Demas and G. Crosby. *J. Phys. Chem.* **75**, 991 (1971).
- 61) G. R. Loppnow, D. Melamed, A. Hamilton, and T. Spiro. *J. Phys. Chem.* **97**, 8957 (1993).
- 62) C. Hansch, A. Leo, and R. Taft. *Chem. Rev.* **91**, 165 (1991).
- 63) Picture obtained from Dr. Kiet Nguyen.

- 64) D. Quimby and F. Longo. *J. Am. Chem. Soc.* **97**, 5111 (1975).
- 65) E. Meyer and D. Cullen, in D. Dolphin (ed.), *The Porphyrins*, Vol. III, Academic Press, New York, 1979, p 516.
- 66) M. Kiemele and S. Schmidt. *Basic Statistics*, Air Academy Press, Colorado Springs, 1993.
- 67) R. Bethea, B. Duran, and T. Boullion. *Statistical Methods*, Marcal-Dekker Inc, New York, 1995, p 123-124.
- 68) D. Shoemaker, C. Garland, and J. Nibler. *Experiments in Physical Chemistry*, McGraw-Hill Inc, New York, 1989, p 35.
- 69) *J. Chem. Phys.*, **82**, 1779 (1985).
- 70) D. Lide. ed. *CRC Handbook of Chemistry and Physics*. 73 ed., CRC Press, Boca Raton, 1992, p 8-49.

VITA

Kirsten Wohlwend was born in Escanaba, Michigan but was raised in Jupiter, Florida. She graduated from Jupiter High School in 1993. She received her Bachelor of Science degree in Biochemistry and her commission as an officer in the United States Air Force from the United States Air Force Academy in 1997. After graduation, she married Lieutenant Christian Wohlwend. Her first official assignment was to Wright State University as a graduate student in chemistry. She completed her Master of Science degree in 1998. Her next assignment will be as a chemist for the Air Force Research Laboratory at Wright Patterson Air Force Base in Dayton, Ohio.